Biobased Chemistry and Technology

Thesis Biobased Chemistry and Technology

Model predictive control of a hybrid renewable energy system in an urban environment

Xun Wang

23-02-2017

WAGENINGEN UNIVERSITY
WAGENINGEN UR

eit Knowledge & Innovation Community
Climate-KIC

Model predictive control of a hybrid renewable system in an urban environment

Name course	:	Thesis project Biobased Chemistry and Technology
Number	:	BCT-80436
Study load	:	36 ects
Date	:	23-02-2017

Student	:	Xun Wang
Registration number	:	921103-927-120
Study programme	:	MBT (Biotechnology)
Report number	:	055BCT

Supervisor(s)	:	Karel Keesman & Yu Jiang
Examiners	:	Karel Keesman, Rachel van Ooteghem & Yu Jiang
Group	:	Biobased Chemistry and Technology
Address	:	Bornse Weilanden 9 6708 WG Wageningen the Netherlands

WAGENINGEN UNIVERSITY

WAGENINGEN UR

Abstract

The accelerated urbanization and steadily growing energy consumption make the urban environments face an unprecedented challenge in utilization of energy. The implementation of hybrid renewable energy system (HRES) and the corresponding management strategy become increasingly important. In this study, three possible configurations of HRES containing micro wind turbines, photovoltaic (PV) cells, a fermentation system and a hydrogen storage module were proposed. By applying model predictive control (MPC) technique, the future disturbances and system behaviours were well understood. Moreover, the fluctuated energy supply caused by PV and wind power modules was complemented by the controllable energy source, bio-hydrogen via anaerobic fermentation. By performing a case study on Slotermeer, Amsterdam, the effectiveness of MPC was validated. A comparison between the merits and deficiencies of three configurations were also presented. The impact of control input on system performance was investigated by sensitivity analysis. Future improvements regarding the economic feasibility and the potential flexibility in HRESs were suggested as well.

Keywords:
Hybrid renewable energy system; Model predictive control; Hydrogen storage; Bio-hydrogen

Contents

Nomenclature

$\beta_{bio,other}$	Economic parameter of otter cost of bio-hydrogen system (€/kg H_2)
$\beta_{consumables}$	Economic parameter of consumables of bio-hydrogen system (€/kg H_2)
$\beta_{electricity}$	Economic parameter of electricity of bio-hydrogen system (€/kg H_2)
β_{el}	Economic parameter of electrolyzer (€/kg H_2)
β_{fc}	Economic parameter of fuel cell (€/kW)
β_{tank}	Economic parameter of hydrogen storage tank (€/kg H_2)
$\beta_{transport}$	Economic parameter of transportation of bio-hydrogen system (€/kg H_2)
β_{water}	Economic parameter of water of bio-hydrogen system (€/kg H_2)
η_{bo}	Efficiency of boost converter
η_{bu}	Efficiency of buck converter
η_{el}	Efficiency of electrolyzer
η_{fc}	Efficiency of fuel cell
η_{NG}	Conversion efficiency between natural gas and electricity
η_{pv}	Efficiency of photovoltaic panels
μ	Specific biomass cell growth rate on glucose (1/h)
μ_{max}	Maximum specific biomass cell growth rate (1/h)
a_{pv}	Area of photovoltaic panels (m^2)
A_{Slot}	Land area of Slotermeer (m^2)
C	Threshold irradiance of photovoltaic panels (kW/m^2)
Cap_{ferm}	Capacity of fermentation tank (L)
$Cap_{storage}$	Capacity of hydrogen storage tank (kJ)
D	Dilution rate (1/h)
d_t	Disturbance input at sampling time t
E_{demand}	Hourly electricity demand (kW)
E_{el}	Electricity consumed by electrolyzer (kW)
E_{fc}	Electricity produced by fuel cells (kW)
E_{pv}	Electricity generated by photovoltaic panels (kW)
E_{reg}	Final electricity consumption on regional level (kJ)
$E_{surplus}$	Electricity surplus (kW)
E_{wt}	Electricity generated by micro wind turbines (kW)
f	Probability of occurrence of a certain wind speed
FOC	Fixed operating cost (€)
FOC_{fc}	Fixed operating cost of fuel cell (€)

G	Glucose concentration in CSTR (g/L)
$G_{0,A}$	Low concentration of glucose in feed (g/L)
$G_{0,B}$	High concentration of glucose in feed (g/L)
G_0	Glucose concentration in feed (g/L)
G_{ING}	Incident irradiance on the photovoltaic panels (kW/m^2)
G_{STC}	Iirradiance at standarde test irradiance (kW/m^2)
$H_{2,bio}$	Cumulative biological H_2 production per liter broth (mol/L)
$H_{2,el}$	Hourly hydrogen produced by electrolyzer (kW)
$H_{2,fc}$	Hourly hydrogen consumed by fuel cell (kW)
$H_{2,tank}$	Hydrogen energy in storage tank (kJ)
h_{hub}	Hub height (m)
h_{ref}	Reference height (m)
I_{ph}	Lower pH inhibition term
Inh_{Slot}	Number of inhabitants in Slotermeer
k	Shape parameter of wind distribution
k_d	Endogeneous rate constant (1/h)
K_G	Monod half saturation constant on glucose (g/L)
k_t	Temperature coefficient (1/$^\circ C$)
$L_{storage,in}$	Initial level of hydrogen storage tank (%)
$L_{storage,LB}$	Lower bound level of hydrogen storage tank (%)
$L_{storage,UB}$	Upper bound level of hydrogen storage tank (%)
$L_{storage}$	Level of hydrogen storage tank (%)
n	Power-law exponent of wind gradient
n_{wt}	Unit number of micro wind turbine
NG_{nat}	Natural gas consumption on national level (kJ)
NG_{reg}	Natural gas consumption on regional level (kJ)
P_{fc}	Total capacity of fuel cell (kW)
P_r	Rated power of micro wind turbine (kW)
P_{STC}	Maximum power at standard test condition[1] (kW/m^2)
P_{wt}	Power generated by wind (kW)
Pd_{H_2}	H_2 produced by bio-hydrogen system (kg H_2)
pH_{LL}	Threshold of completed acid inhibition
pH_{UL}	Upper limit of acid inhibition
q_{HAc}	Specific production rate of acetic acid (mol/g biomass h)
q_{HBu}	Specific production rate of butyric acid (mol/g biomass h)

[1]standard test condition: incident irradiance = 1 kW/m^2, reference temperature = 25 $^\circ C$

$Store_{NG,nat}$	Underground natural gas storage volume on national level (m^3)
$Store_{NG,reg}$	Underground natural gas storage volume on regional level (m^3)
t	Time (h)
$T_{control}$	Control horizon (d)
T_c	Photovoltaic cell temperature ($^\circ C$)
$T_{prediction}$	Prediction horizon (d)
T_r	Reference temperature ($^\circ C$)
$T_{sampling}$	Sampling time interval (d)
$T_{simulation}$	Simulation time (d)
TOC	Total operating cost (€)
TOC_{bio}	Total operating cost of bio-hydrogen system (€)
TOC_{el}	Total operating cost of electrolyzer (€)
TOC_{fc}	Total operating cost of fuel cell (€)
TOC_{tank}	Total operating cost of hydrogen storage tank (€)
TOC_{tot}	Total operating cost of HRES(€)
$u_{t,A}$	Level A of control input
$u_{t,B}$	Level B of control input
u_t	Control input at sampling time t
v_c	Cut-in speed of micro wind turbine (m/s)
v_{hub}	Wind speed at hub height (m/s)
v_o	Cut-out power of micro wind turbine (m/s)
v_{ref}	Wind speed at reference height (m/s)
v_r	Rated speed of micro wind turbine (m/s)
VOC	Variable operating cost (€)
VOC_{bio}	Variable operating cost of bio-hydrogen system (€)
VOC_{el}	Variable operating cost of electrolyzer (€)
VOC_{tank}	Variable operating cost of hydrogen storage tank (€)
X	Biomass concentration (g biomass/L)
$y_{t,max}$	Upper bound of output at sampling time t
$y_{t,min}$	Lower bound of output at sampling time t
y_t	Measured output at sampling time t
$Y_{X/G}$	Biomass yield coefficient on glucose (g biomass/g)

Chapter 1 Introduction

1.1 Background

The constantly growing global energy consumption has already caused concerns on insufficient energy supply, exhaustion of natural resources and severe environmental impacts. The International energy Agency (IEA) published a set of statistical data showing that there was a 102% growth of total final consumption of fuel during the last 40 years (1973-2014) with an average annual increase of 1.8% [1].

The final energy consumption is usually splitted intro three categories which are industry, transportation and other use [2]. Building related energy use including commercial and residential use, which is covered by 'other' sector, has already exceeded the other two major sectors since 2004 [2]. According to Eurostat [3], the residential-related energy consumption took up 25% of overall final energy consumption of EU in 2014. The high percentage was probably due to the fact that the European economy was shifting from heavy industry to service industry [2]. With the economic growth, population explosion, and expansion of urbanization, the building-related energy consumption in European cities will continue to increase in the foreseeable future [4]. Therefore, realizing energy-efficient building clusters is an essential task for European countries.

In order to construct an energy-efficient system for building clusters, there are many angles to look at. Two of them were investigated in this study, which are energy source and supply strategy. In the perspective of energy source, solar and wind power have already been used as alternatives to fossil fuel since the oil crisis of early 1970s owing to their sustainable, non-polluting characteristics. Compared to a diesel engine generator of comparable capacity, although photovoltaic (PV) and wind power systems usually have higher capital investments, the operating and maintenance (O&M) costs are always lower. However, due to the high dependence on meteorological conditions, wind and PV energy cannot be trusted as reliable power for long-term running systems. Considering the merits of wind and PV power, solutions for the energy integration have been raised to compensate their deficiencies [5].

1.1.1 Hybrid renewable energy system (HRES)

The term hybrid renewable energy system (HRES) is used to describe energy systems combining two or more energy sources, at least one of those being renewable energy. The combined energy sources usually can counteract the weaknesses of each other's and enhance system efficiency [6, 7, 8]. Depending on the local availabilities, various renewable energy sources can be integrated in a HRES such as wind, solar, biomass, biogas, hydro power, etc [9]. Besides multiple energy sources, a HRES usually contains a power conditioning equipment, a controller and an optional energy storage system [10]. The conceptual schematic is shown in Figure 1.1.

The performance of various HRESs installed in many countries over the last decade has demonstrated that HRESs can compete with conventional energy systems in the perspectives of stable supply and total life-cycle cost [11, 12, 13, 14, 15].

Although in many current designs, power grids or diesel generators are connected to HRESs as back-up sources to guarantee the stable supply [10]. Many studies have confirmed that 'off-grid' HRESs are economically feasible [16, 17, 18]. To seek a cleaner solution for a sustainable future, 'off-grid' system which is independent from conventional energy sources is apparently a more attractive choice.

1.1.2 Anaerobic fermentation producing hydrogen

Hydrogen energy

Among the various types of energy storage technologies, hydrogen energy is a solution with great potential [19]. Hydrogen is a clean fuel with no CO_2 emissions and has a high energy yield of 143 MJ/kg which is 2.5 times larger than methane (55.6 MJ/kg) [20]. Besides, it can be easily stored chemically or

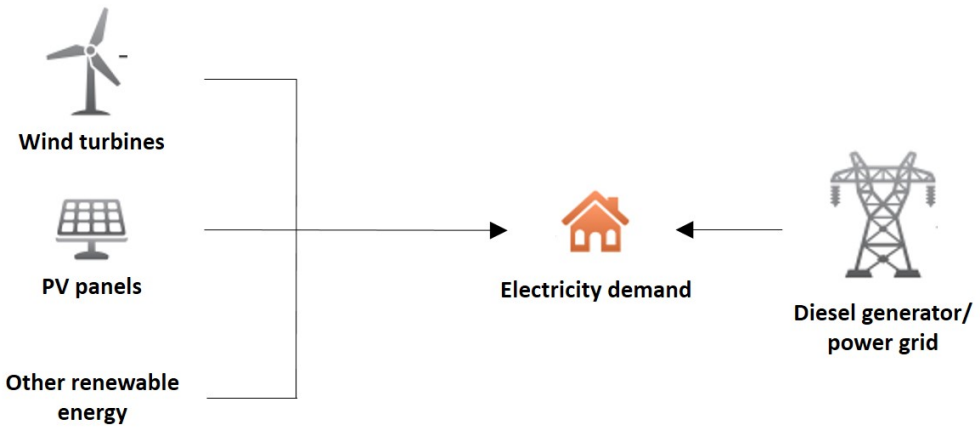

Figure 1.1: The conceptual diagram of HRES

physio-chemically in solid or liquid compounds (metal hydrides, carbon nanostructures, alanates, boro-hydrides, methane, methanol and light hydrocarbons) and be used in fuel cells for electricity generation [21].

In many cases, hydrogen is produced as a by-product of oil refinement [22]. Even though the production cost is low in the current context and the massive production is possible, the extraction from fossil fuels emits loads of greenhouse gasses [22, 23]. Moreover, as a limited resource, the price of fossil fuel will certainly increase in the future. The other route to produce hydrogen is water electrolysis. The reaction is given by [24]:

$$H_2O \longrightarrow H_2 + \frac{1}{2}O_2 \tag{1.1}$$

Electricity is required to force the water (H_2O) molecules to decompose to hydrogen (H_2) and oxygen (O_2) [25]. When the electricity is obtained from an emission-free method such as wind, solar, geothermal, or other renewable energy systems, the water electrolysis can achieve absolutely sustainable hydrogen production [24]. Thus, it makes perfect sense to incorporate hydrogen energy into the HRESs developed in this study. When the wind and solar-based power supply is larger than the demand, the excess electricity can be stored in the form of hydrogen for later use.

Production of bio-hydrogen

Other than the usual power sources mentioned above, biomass resource is also a promising technological option in the renewable hydrogen production. Biomass has been regarded as potentially the world's largest and most sustainable energy source, which comprising 4500 EJ of annual primary production in theory [26]. About 5% of this annual biomass energy alone should cover almost half of the world's total primary energy demand currently [27]. However, in 2007 only 10% of the world primary energy demand was covered by biomass energy [28]. The high availability and low utilization makes it a promising substitute of fossil fuels. Similar to wind and PV power source, using biomass instead of fossil fuels for hydrogen production can reduce greenhouse gases emission significantly [29]. Moreover, biomass source is more controllable than wind and solar power. The controllability of energy stream is of great importance to a HRES with high shares of fluctuating renewable power [30]. The poor performance of solar and wind power in winter seasons can be compensated by the stable biomass energy supply.

Much research is currently focusing on potential methods for hydrogen production from biomass [31]. In general, the available methods can be divided into two categories which are thermochemical and biological routes. Hydrogen can be produced through thermochemical conversion such as pyrolysis, gasification, steam gasification, supercritical water gasification, etc. There are four methods used for biological production: bio-photolysis of water using green algae and blue-green algae ($cyanobacteria$),

photo-fermentation, anaerobic dark fermentation, and two-stage fermentation (integration of dark- and photo-fermentation) [32, 33]. Thermochemical conversion has higher efficiency and lower production cost [34], but the decomposition of feedstocks leads to char and tar formation [35]. Compared to thermochemical process, biological production is found to be more environmental friendly and less energy intensive [36, 37].

A lot of efforts have been made in the bio-based HRES field so far. The studies cover various designs of HRES, which include a HRES of a bio-hydrogen and PV system [19, 38], a HRES of biomass gasification and wind power [39], a PV/biomass gasifier-based hybrid energy system [40], a biomass gasification/solid oxide fuel cell/gas turbine HRES [41], and a hybrid energy system of PV, wind turbine and biogas generator [42]. In this study, a HRES that is more suitable for urban environments consisting of PV panels, micro wind turbines and bio-hydrogen system is proposed.

The bio-hydrogen production method chosen in this study is anaerobic dark fermentation. $Clostridium$, which has been reported as the dominant micro-organisms in anaerobic hydrogen fermentation process [37], ferments hexose to acetic acids, butyric acids with hydrogen and little carbon dioxide as by-products. The superiority of this method is the continuous hydrogen production without photo-energy. The amount of hydrogen produced depends on fermentation pathways, reaction kinetics, fermentation conditions, etc. This leaves more space for the control strategy of HRES [43, 44].

However, there is a major challenge to commercialize dark fermentation technology, which is the high running cost of the system. Several studies have shown that the feasibility of the system mostly depends on the feedstock cost. Usually two types of feedstocks are available for bio-hydrogen production: energy crops, and less expensive residues such as organic residues from municipal wastes, agriculture and forestry, and supermarket leftovers [33, 45]. Sugar-contained organic waste offers an economical option for hydrogen production. At the same time this solves a waste treatment problem for urban areas. In the case study, GFT waste (organic waste in Dutch) produced within the region was proposed as the raw material for anaerobic bio-hydrogen fermentation.

1.2 Problem formulation

Other than a reliable and renewable energy source, an efficient energy management strategy is the other essential to guarantee the robust performance of HRESs. Within the HRES, complexities exist, such as multiple energy streams, various dynamics and technical constraints, and external disturbances including meteorological conditions and real-time electricity demand [46]. The conflict between optimization goals naturally arises when satisfying demand and minimizing cost are being processed at same time. Thus, it is important to anticipate every process and regulate the system in an integrated way.

Optimization based on mathematical modelling assists to solve such complex problems in HRES [5, 47]. To find out the feasible operating solution while handling the trade-offs between performance and cost, plenty of studies have been carried out in modelling and optimization techniques. According to [5], approximately 90% of the studies focus on design and economic aspects. However, a few studies were reported on control methods. It can be expected that HRES will become competitive to conventional power facilities in the near future, so that there is a necessity to investigate the control techniques on energy management which improves the performance and reliability of HRES.

The possibilities of several control strategies applied to HRESs were discussed in a few papers. [48] described a HRES composed of PV, fuel cell, ultra-capacitor systems managed by a classical feedback control strategy. [49],[50] and [51] employed dynamic fuzzy logic control (FLC) for a wind turbine/PV based HRES with energy storage unit to handle the peak power demand. FLC is widely used to deal with uncertainties under the condition where not enough knowledges about the explicit mathematical models are known [50]. Also due to this reason, a FL controller often requires a long time for tuning process [52]. In [53], two control systems were considered for a hybrid energy-storage system. One is a conventional 'state-of-charge' control system that uses the current state of the storage unit for control. The other one presumes knowledge of future demand through feed-forward, neural network or other

artificial intelligence (AI) techniques. Even though AI techniques provide better optimization results [54, 55], they must be provided with historical data of high quality to be efficient [53]. Furthermore, AI also involves intense computations [56, 57] and a long learning process [52].

Need for Model predictive control (MPC)

Among all kinds of control theories, there is one capable of handling various system dynamics, uncertainties, and also easy to synthesize, that is model predictive control (MPC). MPC is designated for a targeting operation to future set-points [58]. It integrates a series of control algorithms that optimize the future response of a system based on an online process model. The major advantages of MPC are the explicit considerations of system dynamics, physical and technical constraints, predictions of future disturbances, and conflicting optimization goals [46].

MPC was originally developed for the refining industry in the late 1970s, and has been established as the core method in advanced process control since the 1990s [46, 59]. Speaking of energy management, the possibilities of implementing MPC have also been discussed in several paper for its ability to deal with constraints in a systematic and straightforward way [47, 59, 60]. [46] proposed a solution for an energy storage with intermittent in-feed from wind and solar power. A MPC strategy is used to alleviate the effects of forecast uncertainties. [59] presented a MPC approach containing a wind power prediction model to smooth the wind power output. [60] designed a novel energy dispatching approach based on MPC for an off-grid HRES system consisting of PV/wind turbine/hydrogen/battery components. In this system, the controller generates the reference power of fuel cell and electrolyzer to satisfy the load power demand and to keep the storage level within their margins.

Based on the work of [60], a further exploration of the MPC application on a novel HRES was done in this thesis work. The application of model predictive control for an off-grid HRES comprising micro wind turbine/PV cell/anaerobic fermentation/hydrogen storage was proposed. The similar HRES configuration was raised by [31] already, yet their study focuses on the general economic analysis but not on energy management or optimization.

1.3 Objective and research questions

The aim of the current research is to develop an optimal energy management strategy based on model predictive control (MPC) for a bio-based hybrid renewable energy system (HRES) in urban environments. To achieve the goal, following research questions need to be answered:

1. What are the possible design configurations of HRES?
2. What are the advantages and disadvantages of different HRES configurations?
3. How does the MPC facilitate the energy management?
4. What are the effects of the glucose concentration in the feed stream on the HRES performance?

A case study of district Slotermeer, Amsterdam is performed based on the historical and field data.

1.4 Outline

The remainder of this thesis is organized as follows. In Chapter 2, methods performed in this study are explained, including the formulation of control problem, the five scenarios discussed in the paper, mathematical models of system components, economic analysis, introduction and implementation of MPC, and the normalized control input sensitivity analysis. In Chapter 3, the data about Slotermeer, the specifications of system components, and the data of natural gas system on national level are presented. Chapter 4 presents the simulation results of HRESs, the sensitivity analysis of control input, the technical and economic comparisons between different HRESs and the comparison about storage sizes between HRESs and natural gas system. Further discussion on the research work is explained in Chapter 5. Finally Chapter 6 concludes the thesis paper and gives directions for future research.

Chapter 2 Method

2.1 Control problem formulation

To help clearly understand the framework of the HRESs proposed in the study, Scenario 1 (Figure 2.1) is used as an example.

The essence of the system is the conversions between two energy carriers, which are electricity and hydrogen. Micro wind turbines and PV panels generate electricity (S) that can be delivered to load power directly ($stream\ 2$) to meet the demand (D). Hydrogen is produced through fermentation ($stream\ 7$) and stored in a storage tank for later use. When demand is less than the generated electricity ($S > D$), the excess wind and solar power ($stream\ 3$) can be used to produce hydrogen through the electrolyzer ($stream\ 4$) and be stored in the form of hydrogen. When there is a shortage in the supply ($S < D$), the stored hydrogen is discharged ($stream\ 5$) and drives hydrogen fuel cells to generate electricity ($stream\ 6$) to compensate the shortage. The storage tank brings a flexibility to the system. Since a strict balance is unrealistic and unnecessary, it allows the stored energy to vary within a safety range. The balances can be described by the following equations:

$$\begin{aligned} S &= stream\ 1 + stream\ 2 \\ D &= stream\ 1 + stream\ 5 \end{aligned} \tag{2.1}$$

$$\left.\begin{aligned} stream\ 1 &= S \\ stream\ 2 &= 0 \\ stream\ 3 &= 0 \end{aligned}\right\} \text{when } S < D \tag{2.2}$$

$$\left.\begin{aligned} stream\ 1 &= D \\ stream\ 4 &= 0 \\ stream\ 5 &= 0 \end{aligned}\right\} \text{when } S \geq D \tag{2.3}$$

$$\begin{aligned} Storage &= stream\ 3 + stream\ 6 - stream\ 4 \\ Storage_{LB} &< Storage < Storage_{UB} \end{aligned} \tag{2.4}$$

where $Storage_{LB}$ and $Storage_{UB}$ are the lower bound and the upper bound of hydrogen storage tank respectively.

The goal of control is to keep hydrogen level in the storage tank within a safety range while the system runs perfectly. In other words, equations (2.1) (2.2) (2.3) (2.4) need to be satisfied at all times. The output of the system is the level of hydrogen storage tank $L_{storage}$ (%). Each of the streams can be regarded as a variable of the system. It is assumed the number of micro wind turbines and the area of PV panels are fixed for the case study which means they are constant parameters. Besides capacities, wind and solar power are dependent on real-time meteorological data. The uncontrollable features of wind speed and solar irradiance make them disturbance inputs (S). Electricity demand is historical data thus it is another disturbance input (D).

According to equations (2.1) (2.2) (2.3) (2.4), $stream\ 1, 2, 3, 4$ and 5 are determined by S and D. Thus $stream\ 6$, hydrogen produced via fermentation, is the only controllable variable. The fermentation system, however, is influenced by plenty of parameters (e.g. strains, temperature, pH, dilution rate, substrate concentration etc.). For the sake of convenience for operation, all these internal parameters

of fermentation are assumed to be fixed except for the glucose concentration in the feed stream which is the control input of this system. Therefore, by manipulating the glucose concentration in the feed, the level of hydrogen storage tank $L_{storage}$, can be kept between $L_{storage,LB}$ and $L_{storage,UB}$.

Three configurations of HRESs are presented below: Scenario 1 (Figure 2.1) is a stand-alone system with no import or export of electricity, and all the renewable energy is stored in the hydrogen tank; The system of Scenario 2 (Figure 2.2) only stores hydrogen from fermentation, and exports extra wind and solar power to the power grid. Scenario 3 (Figure 2.3) is a half measure between the two extreme cases mentioned above, in which half of the excess wind and solar power is stored and the other half is exported to the power grid.

The pros and cons of these three bio-based HRESs can be evaluated by comparison, yet whether the designs are competitive to existing energy systems still need to be studied. Hence, the comparison between the natural gas-based system and the HRESs is also included in the study. Two scenarios involving natural gas were considered: one is the natural gas-only system, in which all the electricity demand is met by natural gas-generated electricity (Figure 2.4); the other one is a HRES where the fermentation system in Scenario 2 is replaced by a natural gas system (Figure 2.5). By comparing the sizes of storage a first judgement can be made.

2.2 Scenarios

2.2.1 HRES scenarios

Scenario 1

The idea of Scenario 1 is to store all the renewable power in the form of hydrogen for later use. The schematic can be found in Figure 2.1.

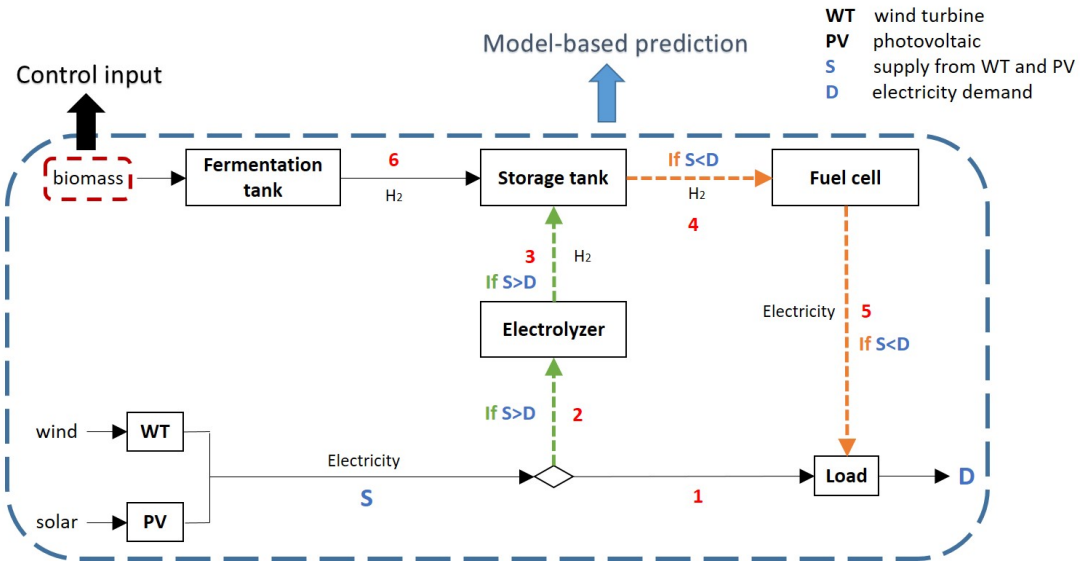

Figure 2.1: Scenario 1 of HRES

The system works in a way that complements seasonal energy supply caused by weather conditions and electricity demands. It stores abundant PV energy during summertime for later use in winter. An off-grid system like this does not rely on power grids or diesel generators, which makes it perfect for remote islands and rural areas where the construction of power grids is challenging, but a large amount of biomass residues are available for fermentation. However, the system is very demanding for the size of equipment because peak PV energy supply requires a huge storage system.

Scenario 2

In this scenario, the excess PV and wind power is directly exported to the power grid system instead of being stored. In this way the size of storage is significantly reduced, and no need for electrolyzers as well (Figure 2.2). Without storing wind and solar power, the bio-hydrogen energy production needs to be

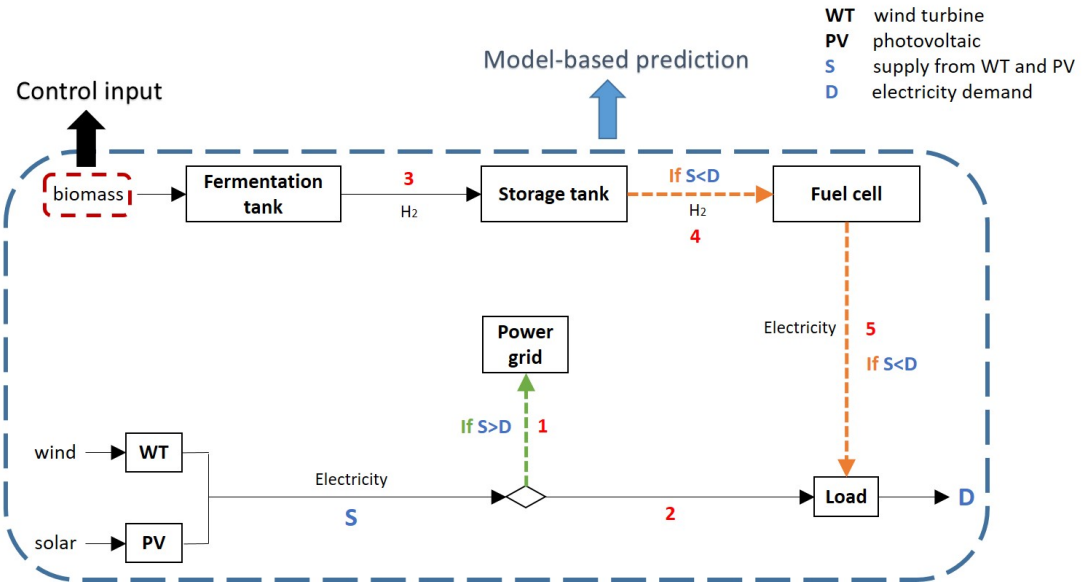

Figure 2.2: Scenario 2 of HRES

more to sustain supply-demand balance. Consequently, more biomass residues and a bigger fermentation tank are required. Besides, a large amount of electricity being exported to power grids during peak hours may cause serious disturbances. Although this is beyond the boundary of this research, it needs to be noted that extra effort is required to handle the issue.

Scenario 3

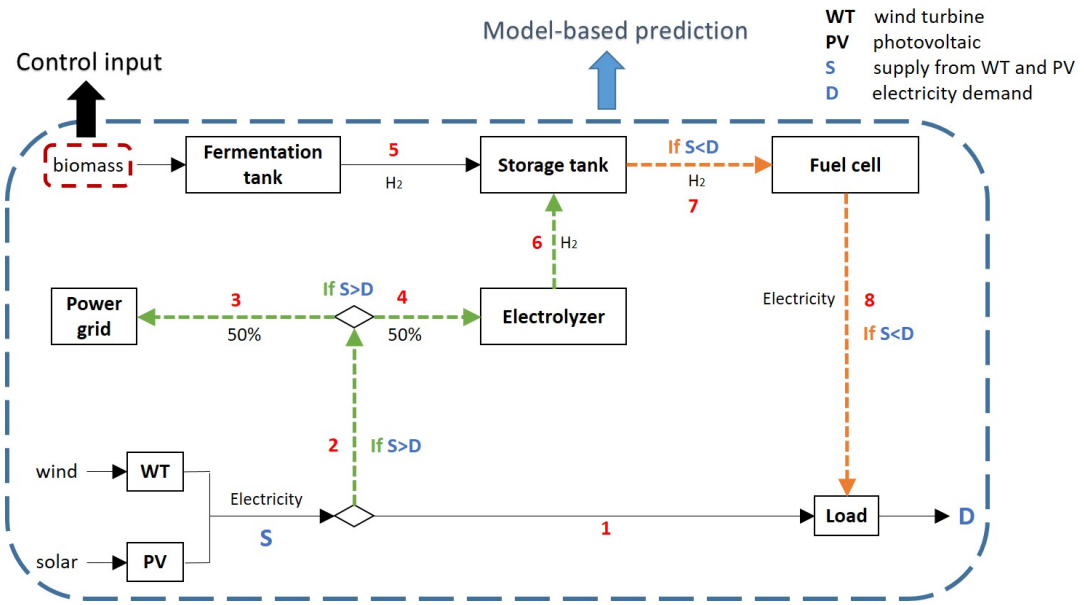

Figure 2.3: Scenario 3 of HRES

The two scenarios described above represent two extreme cases: either storing or exporting the excess wind and PV power. Both solutions have their strengths as well as drawbacks. In order to balance

various aspects, a compromising solution was brought up. In scenario 3, half of the excess PV and wind electricity is exported to power grids, and the other half is stored as hydrogen (Figure 2.3).

2.2.2 HRES vs natural gas related system

Scenario 4

Since the development of HRES is still in research phase, not many data is available to evaluate the feasibility. However, it is still possible to make a preliminary judgement by comparing the HRESs to other energy systems. Natural gas represents 42% of the Netherlands's total primary energy supply which makes it the most important energy source to the Netherlands [61]. And almost 60% of the electricity was generated by natural gas in 2014 [62]. As a dominant energy source of the Netherlands, an energy system powered only by natural gas was chosen as the baseline scenario to compare with the HRESs.

In reality, the natural gas system is a centralized system spreading over several countries, consisting many transportation pipelines and underground storages. To make it possible to be compared with HRES on a district level, the natural gas system was scaled down linearly based on the ratio between national and regional electricity consumptions.

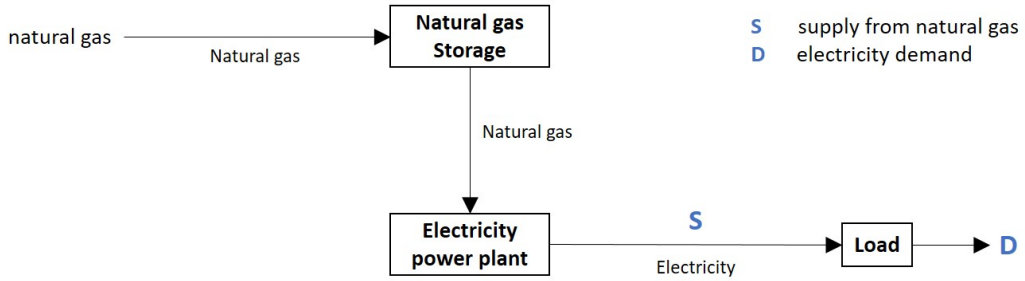

Figure 2.4: Scenario 4 of natural gas-based system

It is assumed that the natural gas coming from national pipeline (Figure 2.4) is stored in a local underground cavern. When needed, the stored natural gas is converted to electricity through an electricity power plant.

Scenario 5

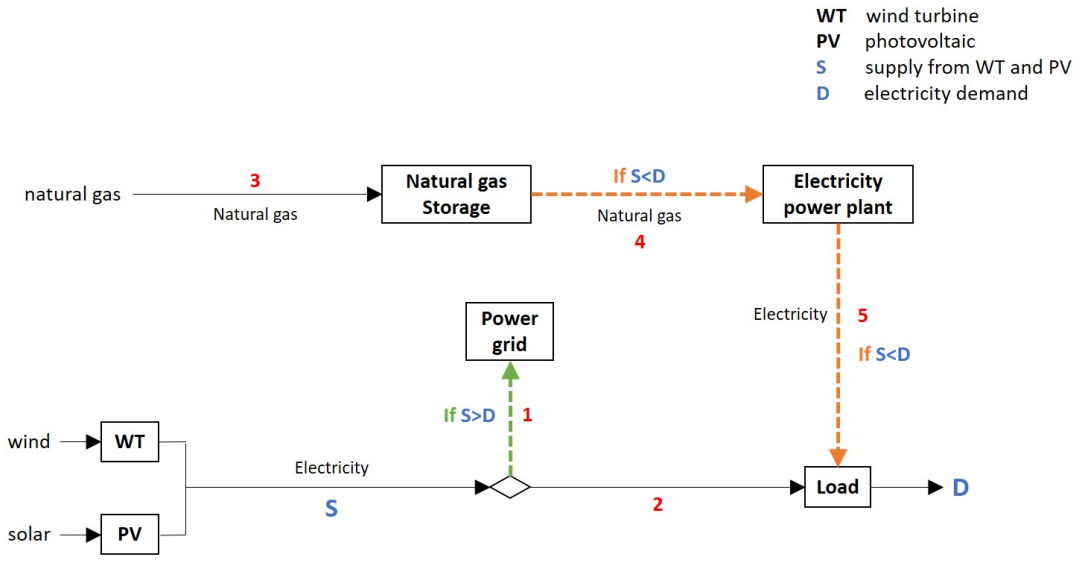

Figure 2.5: Scenario 5 of natural gas-based system

In the last scenario (Figure 2.5), natural gas system replaces the hydrogen system in scenario 2. Linear scaling down was also applied in this scenario. By comparing scenario 5 and 2, it can be concluded whether hydrogen is better as an energy carrier than natural gas is, and whether hydrogen fermentation system is competitive compared to the natural gas system.

2.3 Modelling of system components

In this section, mathematical models for each component of HRES are presented. The approach of scaling down the natural gas system from national level to local level is also explained in the end of the section.

Due to the data limitation and practical purpose, the optimization was conducted for 1-year simulation with a time interval of 1 hour. Hence the inputs/disturbances/outputs are constant within one hour.

2.3.1 Electricity demand

The electricity demand E_{demand} (kW) was simulated based on the hourly statistical data of 2014 in Slotermeer, Amsterdam which is provided by Alliander as a project partner.

2.3.2 Model for wind power system

The following model is adopted for the simulation of wind-generated power P_{wt} (kW) [63]:

$$P_{wt} = \begin{cases} 0 & v_{hub} < v_c \\ P_r \, \dfrac{{v_{hub}}^2 - {v_c}^2}{{v_r}^2 - {v_c}^2} \, n_{wt} & v_c \leq v_{hub} \leq v_r \\ P_r \, n_{wt} & v_r \leq v_{hub} \leq v_o \\ 0 & v_{hub} > v_o \end{cases} \tag{2.5}$$

where v_{hub} (m/s) is the wind speed at the hub height of wind turbine; n_{wt} is the unit number of micro wind turbines; P_r (kW), v_r (m/s) v_c (m/s), and v_o (m/s) are specifications of wind turbine model types, which are rated power, rated speed, cut-in speed and cut-out speed respectively.

Wind speed is highly affected by ground surface friction. The wind speed becomes slower when it gets closer to ground [64]. Due to the fact that the wind measuring point usually does not have the same height as the wind turbine does, the measured wind speed data cannot be used directly in the model. To estimate the actual wind speed at hub height of wind turbines, the available measured wind data can be adjusted by using a power-law relation:

$$\left(\frac{v_{hub}}{v_{ref}}\right) = \left(\frac{h_{hub}}{h_{ref}}\right)^n \tag{2.6}$$

where v_{hub} (m/s) is the wind speed at a given hub height (distance between the centre of turbine and ground) h_{hub} (m); v_{ref} (m/s) is the wind speed at reference height h_{ref} (m); n is the power-law exponent which is often taken as $\frac{1}{7}$ [65].

Hourly wind speed data are not accurate enough since the wind is not steady within an one-hour interval. Therefore, the Weibull distribution is used to estimate the probability of occurrence of a certain wind speed $f(v_{hub})$ [66, 67, 68]:

$$f(v_{hub}) = \frac{k\sqrt{\pi}}{2 \cdot v_{hub}} \left(\frac{\sqrt{\pi}}{2}\right)^{k-1} e^{-\left(\sqrt{\pi}/2\right)^k} \tag{2.7}$$

where shape parameter k is typically taken as 2. A typical probability of occurence of wind speed at the hub height $f(v_{hub})$ distribution is shown in Figure 2.6.

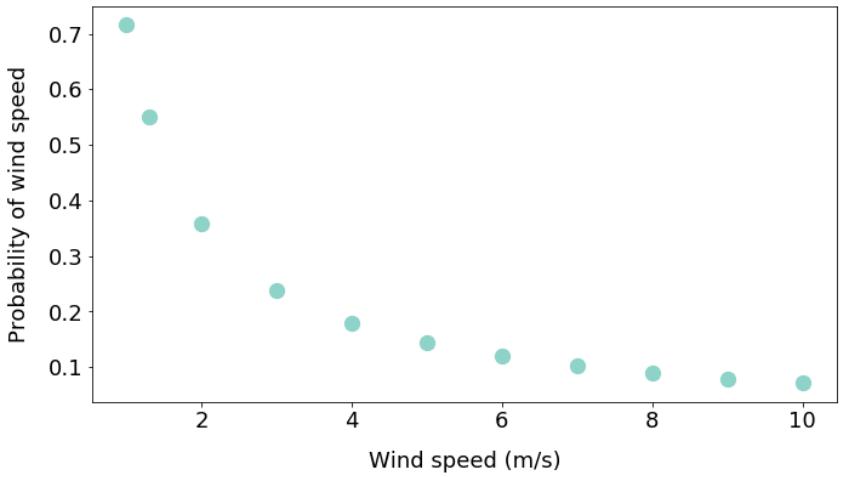

Figure 2.6: Wind speed Weibull distribution

The electricity generated by micro wind turbines E_{wt} (kW) can be presented by the following expression [64]:

$$E_{wt} = f(v_{hub})\ P_{wt}(v_{hub}) \tag{2.8}$$

2.3.3 Model for photovoltaic energy system

To simulate the performance of photovoltaic panels, the following model was used to calculate electricity produced by solar irradiance E_{pv} (kW) [69]:

$$E_{pv} = \begin{cases} 0 & G_{ING} \leq C \\ P_{STC}\ \dfrac{G_{ING}}{G_{STC}}\ (1 + k_t\ (T_c - Tr))\ a_{pv} & G_{ING} > C \end{cases} \tag{2.9}$$

When the incident irradiance G_{ING} (kW/m^2) shed on PV cells is less than the threshold irradiance C (kW/m^2), no solar power is produced. Otherwise solar-generated power is determined by irradiance G_{ING}, cell temperature T_c ($^\circ C$), area of PV a_{pv} (m^2), and characteristics of the PV cell including P_{STC}, G_{STC} (kW/m^2), k_t (1/$^\circ C$), C (kW/m^2).

The maximum power at standard condition P_{STC} (kW/m^2) can be calculated by eq.(2.10) with PV cell efficiency η_{pv} [64] :

$$P_{STC} = \eta_{pv}\ G_{STC} \tag{2.10}$$

2.3.4 Energy balance

So far the electricity supply comes from micro wind turbines E_{wt} and photovoltaic panels E_{pv}. However, it is highly dependent on weather and seasonal conditions. Certainly there is a gap between supply and demand E_{demand}, which is named 'electricity surplus' $E_{surplus}$ (kW) in this research:

$$E_{surplus} = E_{wt} + E_{pv} - E_{demand} \tag{2.11}$$

2.3.5 Bio-Hydrogen energy system

Kinetic model for dark fermentation

Hydrogen production via anaerobic fermentation comes with the formation of acetic acid and butyric acid as major metabolites [70, 71]. The stoichiometric formulas [72] are shown below:

$$\overbrace{C_6H_{12}O_6}^{glucose} + 2H_2O \longrightarrow 2\overbrace{CH_3COOH}^{acetic\ acid} + 2CO_2 + 4H_2 \tag{2.12}$$

$$\overbrace{C_6H_{12}O_6}^{glucose} \longrightarrow \overbrace{C_3H_7COOH}^{butyric\ acid} + 2CO_2 + 2H_2 \tag{2.13}$$

The fermentation process is simulated as a continuous stirred-tank reactor (CSTR) system. Several kinetic models based on material balances were developed to describe the steady-state behaviour of (1) formation of biomass, (2) consumption of substrate and (3) production of hydrogen.

Combining endogenous metabolism [73] and acid inhibition caused by the formation of volatile fatty acids (VFAs), the general material balance equations [74, 75] can be written as follows:

For biomass formation,

$$\frac{dX}{dt} = \mu X I_{pH} - (D + k_d)X \tag{2.14}$$

where X is the biomass concentration (g biomass/L); μ is the specific growth rate on glucose ((1/h)); I_{pH} is the pH inhibition term; D is the dilution rate (1/h); k_d is the endogenous metabolism (1/h).

For glucose consumption:

$$\frac{dG}{dt} = D(G_0 - G) - \frac{1}{Y_{X/G}}(\mu X I_{pH} - k_d X) \tag{2.15}$$

where G is the glucose concentration in CSTR (g/L); G_0 is the glucose concentration in the feed (g/L); $Y_{X/G}$ is the biomass yield on glucose (g biomass/g).

The Monod equation [74] was used to fit cell growth. The specific cell growth rate on glucose is defined as [73]:

$$\mu = \frac{\mu_{max} G}{K_G + G} \tag{2.16}$$

where μ_{max} is the maximum specific cell growth rate (1/h), and K_G is the Monod half saturation constant on glucose (g/L).

The formation of VFAs is assumed to be growth-associated [73]. Hydrogen is always produced coupled with VFAs formation in a fixed stoichiometric ratio. Therefore, the differential equation of hydrogen production can be expressed as:

$$\frac{d(H_{2,bio})}{dt} = 2 \cdot q_{HAc}X + 2 \cdot q_{HBu}X \tag{2.17}$$

where $H_{2,bio}$ is the cumulative H_2 production per broth volume (mol/L); q_{HAc} and q_{HBu} (mol/g biomass h) denote specific production rates of acetic acid and butyric acid respectively. The factor of 2 is taken based on the stoichiometric relations (eq. (2.12)(2.13)).

According to the Anaerobic digestion model No.1 (ADM1) [76], the empirical lower pH inhibition term I_{pH} is defined as:

$$I_{pH} = \begin{cases} 1 & pH \geq pH_{UL} \\ exp[-3\left(\frac{pH - pH_{UL}}{pH_{UL} - pH_{LL}}\right)^2] & pH < pH_{LL} \end{cases} \tag{2.18}$$

where pH_{UL} and pH_{LL} denote the upper limit at which the bacteria are not inhibited, and the lower limit at which complete inhibition occurs. The reference values of pH_{UL} and pH_{LL} are pH 5.5 and pH 4 respectively [76]. However, as the focus of this research is on energy dispatch instead of fermentation, pH is assumed to be controlled always around 7. Thus, the term I_{pH} is assumed to be close to 1.

Conversion between glucose and GFT waste

The kinetic models described above use glucose as the substrate. GFT waste (organic waste in Dutch) has been proposed as the substrate source in this study. In the research of [44], a high hydrogen production potential of 180 ml H_2/g TVS (total volatile solid) was achieved. An adjusted organic faction of municipal solid waste (OFMSW) composed of GFT waste was used as the substrate and was fermented with night soil sludge and sewage sludge. According to [77], yields of 3.2 mol H_2/mol hexose were obtained which is comparable to the result from [44].

A basic assumption in this study is that the two results are comparable. Because the two results are in different units, which involve hexose and TVS, a quantitative link between hexose and GFT waste can be bridged. To simplify the situation, hexose was assumed to be glucose. As a result, approximately 0.2723 g glucose is contained in 1 g GFT waste. The detailed calculation can be found in Appendix C.

2.3.6 Hydrogen storage system

Electrolyzer

According to the energy balance calculation eq (2.11), when the value of $E_{surplus}$ is positive, there is an excess power generated by wind and solar, which can be used in water electrolysis to produce hydrogen. The electricity consumed by electrolyzer E_{el} (kW) is presented by the following equation:

$$E_{el} = \begin{cases} 0 & E_{surplus} \leq 0 \\ E_{surplus} & E_{surplus} > 0 \end{cases} \tag{2.19}$$

The procedure of electrolysis can be represented by a power source (the buck converter) feeding the power needed by the electrolyzer [49]. Since both buck converter and electrolyzer have quite complicated dynamics, they were both modelled as ideal components with fixed efficiencies for simplicity. Thus, hourly hydrogen produced by electrolyzer $H_{2,el}$ (kW) is described as:

$$H_{2,el} = \begin{cases} 0 & E_{surplus} \leq 0 \\ E_{surplus}\,\eta_{bu}\,\eta_{el} & E_{surplus} > 0 \end{cases} \tag{2.20}$$

where η_{bu} and η_{el} are efficiencies of the buck converter and the electrolyzer.

Fuel cell

When $E_{surplus}$ is negative the shortage of electricity can be compensated by hydrogen fuel cells. This part consists of a hydrogen fuel cells and a boost converter, which is very similar to the buck converter & electrolyzer group. The same simplification was done for the efficiencies of the boost converter and the fuel cell.

The electricity generated by the fuel cell E_{fc} (kW) is described as:

$$E_{fc} = \begin{cases} 0 & E_{surplus} \geq 0 \\ -E_{surplus} & E_{surplus} < 0 \end{cases} \tag{2.21}$$

Hourly hydrogen utilized by the fuel cell $H_{2,fc}$ (kW) is described as:

$$H_{2,fc} = \begin{cases} 0 & E_{surplus} \geq 0 \\ \dfrac{-E_{surplus}}{\eta_{bo}\,\eta_{fc}} & E_{surplus} < 0 \end{cases} \tag{2.22}$$

where η_{bo} and η_{fc} are efficiencies of the boost converter and the fuel cell.

Hydrogen balance in storage tank

As shown in Figure 2.1, the balance in the hydrogen storage tank can be presented as below:

$$\frac{d(H_{2,tank})}{dt} = H_{2,el} + H_{2,bio} - H_{2,fc} \tag{2.23}$$

where $H_{2,tank}$ (kJ) is the energy stored in the storage tank; t (s) is the time.

2.3.7 Natural gas system

Natural gas consumption

During the transformation from natural gas to electricity, only part of the energy is valid due to the efficiency loss. The regional natural gas consumption NG_{reg} (kJ) can be calculated by:

$$NG_{reg} = \frac{E_{reg}}{\eta_{NG}} \tag{2.24}$$

where E_{reg} is the final electricity consumption on regional level (kJ), and η_{NG} is the conversion efficiency.

Storage estimation

Due to the fact that natural gas supply involves both transportation and storage, it is too complicated for this study to get deep into natural gas systems. Therefore, a rough calculation was made to estimate

the natural gas storage volume.

It is assumed that the natural gas storage system is linearly correlated to the natural gas consumption. Thus, the regional natural gas storage volume $Store_{NG,reg}$ (m^3) can be estimated by:

$$Store_{NG,reg} = \frac{NG_{reg}}{NG_{nat}} \; Store_{NG,nat} \tag{2.25}$$

where NG_{nat} (kJ) is the national natural gas consumption; $Store_{NG,nat}$ (m^3) is the national natural gas storage volume.

2.4 Economic analysis

The total operating cost of the HRES is part of the MPC's cost function.

2.4.1 Operating cost

For the same scenario, there could be multiple feasible operating solutions. For example, 15 g glucose/L and 20 g glucose/L in the feed stream could both make the system run successfully. However, the optimal solution is the one with the lowest total cost. The capital cost is fixed because the size of the system remains the same, but the operating cost varies as operating conditions change. Therefore, to obtain the optimal solution of each scenario, operating cost was used as an important variable in model predictive control, which is presented in the following section.

There are two types of operating cost which are variable operating cost VOC and fixed operating cost FOC. Variable operating costs are calculated based on material balances from the process model. Fixed operating costs are estimated from manpower requirement, maintenance, capacities of system facilities of similar size [78]. The variable and fixed operating cost can be added up to the total operating cost TOC:

$$TOC = VOC + FOC \tag{2.26}$$

Operating cost of wind & photovoltaic power systems

It is assumed that micro wind turbines are operated at its rated power P_r (kW) over the year, therefore the operating cost of the wind power system can be regarded as fixed. The same assumption was made for PV power system, in which the PV panels generate power in its maximum capacity at standard test conditions P_{STC} (kW). This means as long as the systems are running, the operating cost per unit is fixed.

Therefore, for both wind and PV power systems, the variable operating costs VOC can be taken as 0:

$$VOC_j = 0 \tag{2.27}$$

where the subscript j denotes wind power system or PV power system.

And the fixed operating costs FOC are described as:

$$FOC_j = P_j \; n_j \; \beta_j \tag{2.28}$$

where n_j represents the unit number of micro wind turbines or the area of PV panels; β_j is the economic parameter of micro wind turbines or PV panels (€/kW).

The total operating cost of wind PV power system TOC_j is:

$$TOC_j = P_j \, n_j \, \beta_j \text{ , with } \; j = \{wt, \, pv\} \tag{2.29}$$

Operating cost of bio-hydrogen system

Operating costs of the bio-hydrogen system is more complicated. According to the data from [79], operating costs of fermentation are all related to hydrogen production. Therefore, the total operating cost TOC_{bio} was taken as variable VOC_{bio}:

$$TOC_{bio} = VOC_{bio} = (\beta_{electrity} + \beta_{water} + \beta_{consumables} + \beta_{transport} + \beta_{bio,other}) Pd_{H_2} \tag{2.30}$$

where $\beta_{electricity}$, β_{water}, $\beta_{consumables}$, $\beta_{transport}$ and $\beta_{bio,other}$ represent the economic parameters (€/kg H_2) of electricity, water, consumables, transportation and other costs during fermentation. Pd_{H_2} refers to the hydrogen produced through fermentation (kg H_2).

Operating cost of electrolyzer

The total operating cost of electrolyzer TOC_{el} is also considered as variable operating cost VOC_{el}:

$$TOC_{el} = VOC_{el} = \beta_{el} \, Pd_{H_2} \tag{2.31}$$

where β_{el} is the economic parameter of electrolyzer (€/kg H_2); $Pd_{\,bio}$ is the hydrogen produced through fermentation (kg H_2).

Operating cost of fuel cell

The calculation of operating cost of fuel cell is based on its capacity, therefore the fixed operating cost FOC_{fc} equals to the total operating cost TOC_{fc}:

$$TOC_{fc} = FOC_{fc} = P_{fc} \, \beta_{fc} \tag{2.32}$$

where P_{fc} is the total capacity of fuel cells (kW); β_{fc} is the economic parameter of fuel cells (€/kW).

Operating cost of hydrogen storage tank

Since the hydrogen storage tank is under a pressure of 30 bar, hydrogen needs to be compressed before being stored. The electrolyzers produce compressed hydrogen, thus only hydrogen produced by fermentation needs an extra compression process [80]. The major operating cost of hydrogen storage tank is on gas compression, which means it is a variable cost VOC_{tank} related to the bio-hydrogen production Pd_{H_2}.

$$TOC_{tank} = VOC_{tank} = \beta_{tank} \, Pd_{H_2} \tag{2.33}$$

where β_{tank} is the economic parameter of hydrogen storage tank (€/kg H_2).

Total operating cost

The total operating cost TOC_{tot} is the addition of operating costs of all components. Due to the different system design, the TOC_{tot} of scenario 2 has a slight difference to those of scenario 1 and 3:

For Scenario 1 & 3:

$$TOC_{tot} = TOC_{wt} + TOC_{pv} + TOC_{bio} + TOC_{el} + TOC_{fc} + TOC_{tank} \tag{2.34}$$

For Scenario 2:

$$TOC_{tot} = TOC_{wt} + TOC_{pv} + TOC_{bio} + TOC_{fc} + TOC_{tank} \tag{2.35}$$

2.5 Model predictive control (MPC)

Model predictive control (MPC) is an optimal control based strategy [81] which uses an explicit dynamic model to find the optimal control inputs that force the output to follow the best predicted behaviour of the system over a prediction horizon [82].

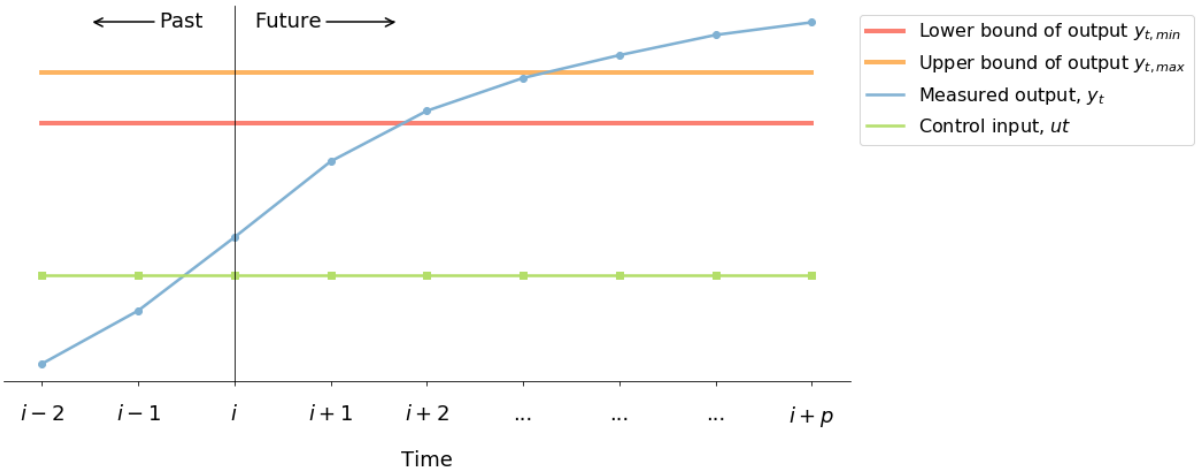

Figure 2.7: Control problem

Taking Figure 2.7 as an example, without adding any controls the control input u_t keeps constant before and after current time i ($i = 2, 3, 4, ..., n$). The measured output y_t starts from low level and exceeds the constraints between $y_{t,min}$ and $y_{t,max}$ quickly. The goal of MPC is to maintain the measured output y_t within the allowable range $y_{t,min} \leq y_t \leq y_{t,max}$ by changing the control input u_t.

MPC is a specific receding horizon control method which is illustrated in Figure 2.8(a) and 2.8(b). It is assumed that the sampling time interval equals to 1. The lengths of prediction horizon is p ($1 \leq p$). At current time i ($i = 2, 3, 4, ..., n$), the MPC controller firstly makes predictions on control inputs u_{i+1}, u_{i+2}, ..., u_{i+p} over a prediction horizon p in the future to make the measured outputs, y_{i+1}, y_{i+2}, ..., y_{i+p}, stay in the range of $[y_{i,min}, y_{i,max}]$. But only the first move u_{i+1}, is implemented to the system.

As time horizon moves one step forward, new measurement of y_{i+1} at time $i + 1$ is obtained. Because of the uncertain disturbance inputs d_t, some deviations between measured and predicted outputs are expected. Then, based on the new measurement y_{i+1}, a new predictions of the control input u_{i+2}, u_{i+3}, ..., u_{i+p+1} and the output y_{i+2}, y_{i+3}, ..., y_{i+p+1} are done. Afterwards the same procedure is repeat every time time horizon moves until the simulation ends.

2.5.1 Numerical solution

Enumeration is employed to solve the MPC problem in this study. The control input u_t only has 2 levels, low-level and high-level denoted by $u_{t,A}$ and $u_{t,B}$. At each sampling time, control input enters the system only as a constant ($u_{t,A}$ or $u_{t,B}$) but time varying parameter [83]. For instance, at a prediction

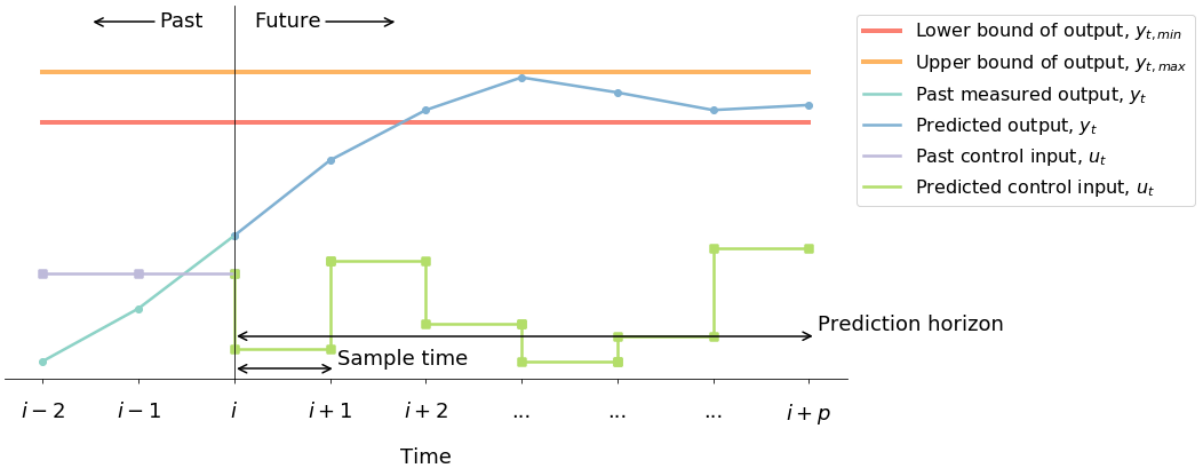

(a) MPC at time i

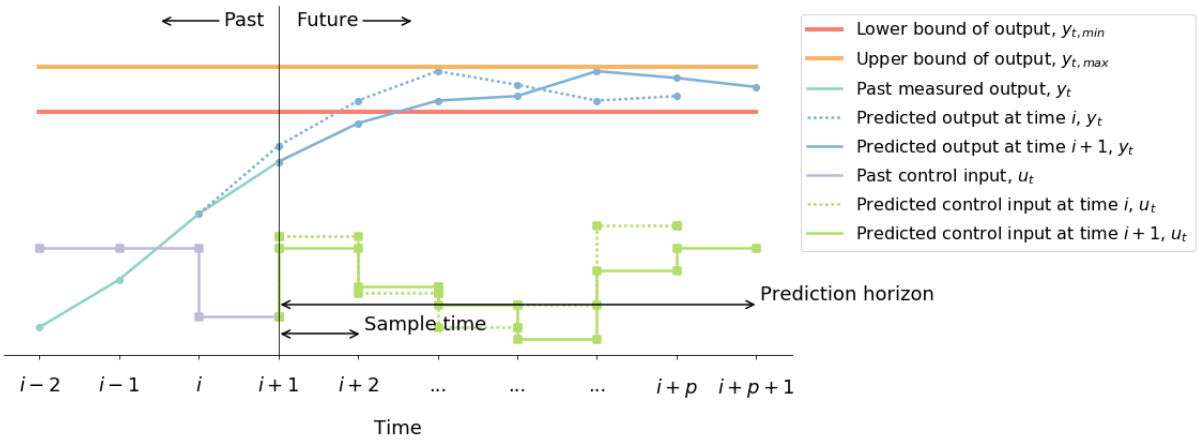

(b) MPC at time $i+1$

Figure 2.8: MPC principles

horizon from time i to $i+p$ with a control horizon from i to $i+c$ ($c \leq p$), each of the control inputs within the control horizon (u_i, u_{i+1}, ..., u_{i+c-1}) can be either $u_{t,A}$ or $u_{t,B}$. The inputs beyond the control horizon (u_{i+c}, u_{i+c+1}, ..., u_{i+p-1}) remain the same as u_{i+c-1}. Therefore, 2^c different combinations of u_i, u_{i+1}, ..., u_{i+p-1} can be obtained for one prediction horizon. Then the combination that makes y_i, y_{i+1}, ..., y_{i+p-1} stay in $y_{t,min} \leq y_t \leq y_{t,max}$ and with the minimum cost function is selected as the optimal control inputs.

There are two main reasons why enumeration is more suitable for this case study than a search-based solution. First, enumeration significantly reduces the computation time [84]. Due to the presence of fermentation system which is relatively slow, the prediction horizon has to be long enough to predict its potential behaviours. Such a long prediction horizon will lead to massive computations for a search-based method. By performing enumeration, the optimal solution can be obtained through the selection among limited combinations. Moreover, the result from a search-based solution might be too complicated in actual practice. The two-level input leads to much convenience.

2.5.2 Set-up of MPC controller

The controller setup is described as below:

the simulation time (d):

$$T_{simulation} = 365$$

the sampling time interval (d):

$$T_{sampling} = 1$$

the control horizon (d):

$$T_{control} = 4$$

the prediction horizon (d):

$$T_{prediction} = 14$$

System variables

For all three HRESs discussed in the study, the system variables are listed as below:

y_t Outputs

$L_{storage}$	Level of hydrogen storage tank (%)

u_t Control inputs

G_0	Glucose concentration in feed (g/L)

d_t Disturbance inputs

v_{hub}	Wind speed at hub height (m/s)
T_c	PV cell temperature ($^\circ C$)
G_{ING}	Irradiance on PV cells (kW/m^2)
E_{demand}	Electricity demand (kW)

Objective and constrains

The objective of MPC controller is minimizing the cost function. The cost function described below is applicable to the systems in Scenario 1, 2 and 3. However, it should be noted that the total operating cost TOC_{tot} varies from different scenarios because of changes in system size and design (See eq. (2.34) and (2.35)).

$$J = \begin{cases} \sum_{t=i}^{i-1+T_{prediction}} TOC_{tot}(u_t) & 0 \leq i < 240 \\ \underbrace{\left(\sum_{t=i}^{i-1+T_{prediction}} TOC_{tot}(u_t)\right)}_{\text{term 1: sum of operating cost}} + \underbrace{\alpha \cdot \left(y_{(t=i-1+T_{prediction})} - y_{(t=0)}\right)^2}_{\text{term 2: penalty on terminal cost}} & 240 \leq i \leq 351 \end{cases} \tag{2.36}$$

subject to the constraints on control input and output:

$$u_t \in \{u_{t,A}, u_{t,B}\} \tag{2.37}$$

$$y_{t,min} \leq y_t \leq y_{t,max} \tag{2.38}$$

where t is the sampling time; i is the current prediction time; u_t is the control input; y_t is the system output; TOC_{tot} is the total operating cost; $T_{prediction}$ is the length of prediction horizon (d); α is the

weighting factor; $u_{t,A}$ and $u_{t,B}$ are the low- and high-level of control input; $y_{t,min}$ and $y_{t,max}$ are the lower bound and the upper bound of output y_t.

From January to August, the cost function only depends on total operating cost over each prediction horizon. It means as long as the storage level is in the safety range the controller would choose the solution with the lowest operating cost. In order to run the system for several subsequent years, the storage at the end of the year needs to be reset to a comparable level to the initial storage at the beginning of the year. Thus, a penalty term is added to the cost function when $i \geq 240$.

2.6 Normalized control input sensitivity analysis

At the early stage of the simulation so far, the two levels of control input $u_{t,A}$ and $u_{t,B}$ were pre-defined based on the result of [85]. However, the result from other's work is not necessarily applicable to the different model developed in this study. In order to provide an evaluation of the confidence in the pre-defined control input, a normalized sensitivity analysis of control input on several system outcomes was performed.

$u_{t,A}$ is designed as a value close to 0 which merely supports the growth of micro-organisms to be in balance with the endogenous decay. $u_{t,B}$ is a higher value that is favourable for biomass to grow and produce. In fact the two-level input strategy mimics a situation where either zero production or high production occurs. In this case it is unnecessary to perform a sensitivity analysis on the low-level $u_{t,A}$ but on the high-level u_B only.

In order to evaluate the relative effects of the $u_{t,B}$ on different outcomes y, a dimensionless sensitivity coefficient S is introduced, that is [86]:

$$S_j = \frac{u_{B,j}}{y_j} \frac{\partial y_j}{\partial u_{B,j}} \tag{2.39}$$

where subscript j denotes different test scenarios. $u_{B,j}$ is the control input and y_j is the corresponding outcome. Each of the $u_{B,j}$ is then perturbed by a fixed variation (e.g. ± 5% of $u_{B,j}$). The perturbation around $u_{B,j}$ is indicated by $\partial u_{B,j}$. The variation of y_j is represented by ∂y_j.

There are two main criteria for selecting the range of $u_{B,j}$. First, the baseline value should be included which in this case is pre-defined $u_{t,B}$; second, the selections should be realistic. Thus, the control input which is the glucose concentration in feed for test scenarios should be able to provide reasonable condition for biomass growing and producing. According to [87, 85], the test range is decided to be [20, 30] (g/L) which is the optimal glucose concentration for hydrogen production.

Chapter 3 Case Study & data collection

The developed models of the HRES was applied to the district Slotermeer, Amsterdam. The simulation was performed based on the real historical meteorological and field data of 2014 [1]. In this chapter, the obtained data source and related plottings, the specification parameters of the HRESs, the data of national natural gas system are presented.

3.1 Field and historical data

3.1.1 Hourly electricity demand of 2014

The hourly electricity demand E_{demand} was modelled based on the statistical data of 2014 in Slotermeer which is provided by Alliander as a project partner. The according plotting Figure A.1 is presented in Appendix A.

3.1.2 Hourly wind speed and solar irradiance of 2014

The hourly wind speed, solar irradiance and temperature data were obtained from Koninklijk Nederlands Meteorologisch Instituut (KNMI) [88]. The observation station is located at Schiphol. The hourly reference wind speed v_{ref} and incident solar irradiance G_{ING} data are plotted in Figure A.2 and Figure A.3 respectively which can be found in Appendix A. The measurement point of wind is assumed to be 10 m high ($h_{ref} = 10$ m).

3.1.3 Specifications of Slotermeer

Some information about Slotermeer is needed for the case study. The investigated zone belongs to Amsterdam Nieuw-west with the population of 146,700 [89] and the land area of 32.38 km^2 [90]. Slotermeer takes up about 2/3 of the total area of Nieuw-west. It is assumed that the population is distributed evenly within Nieuw-west, thus the land area A_{Slot} and the inhabitants Inh_{Slot} can be calculated as 21.59 km^2 and 97,800 respectively.

To estimate the potential GFT wastes production in Slotermeer, the average data of the Netherlands was used. In 2014, 527 kg/capita municipal wastes are generated [91], of which 38% are GFT wastes [92]. So that the annual GFT production in Slotermeer is assumed to be calculated as 97,800$\times$527$\times$0.38 = 19,585,428 kg = 19,586 ton.

3.2 Characteristic parameters of systems

The HRES is composed of multiple component models as elaborated in Chapter 2. The specifications of these components are necessary for system modelling and optimization. Table 3.1 lists all characteristic parameters of the components and system parameters applied in this thesis.

[1] All data applied in the study are of year 2014 without specific indications

Table 3.1: Component characteristic and system parameters

Component	Parameter	Value *	Unit
Micro wind turbine	P_r	2.4 [93]	kW
	v_r	10.3 [94]	m/s
	v_c	3.2 [95]	m/s
	v_o	63 [93]	m/s
	n_{wt}	8,000 [a]	-
	h_{hub}	40 [b]	m
	h_{ref}	10 [c]	m
Photovoltaic panel	G_{STC}	1 [96]	kW/m^2
	C	0.05 [d]	kW/m^2
	k_t	-0.0045 [97]	1/$^\circ$C
	a_{pv}	460,000 [a]	m^2
	T_r	25 [96]	$^\circ$C
	η_{pv}	0.154 [98]	-
Dark fermentation	D	1/12 [99, 100, 73]	1/h
	k_d	0.02	1/h
	$Y_{X/G}$	0.15 [101]	g biomass/g
	μ_{max}	0.172 [100]	1/h
	K_G	0.0637 [e]	g/L
	q_{HAc}	0.003	mol/g biomass h
	q_{HBu}	0.0021	mol/g biomass h
	I_{pH}	1 [f]	-
Electrolyzer	η_{bu}	95% [50]	-
	η_{el}	80% [102]	-
Fuel cell	η_{bo}	95% [50]	-
	η_{fc}	60% [103]	-

* The parameters without references and footnotes are the reasonable assumptions made based on various literatures.

[a] Based on the results of [64], the maximum n_{wt} and a_{pv} are 10,000 and 842,500 respectively. In this study, 8,000 and 460,000 are taken as the values of n_{wt} and a_{pv}.

[b] The h_{hub} is calculated based on the average height of buildings in Amsterdam which is 30 m [104] and the tower height of the micro wind turbines which is approximately 10 m [94].

[c] See Section 3.1.2.

[d] The threshold irradiance C is taken as 5% of G_{STC}.

[e] The K_G is converted from 68 mg COD/L [100] (1 g glucose = 1.0667 g COD).

[f] See Section 2.3.5.

3.3 Natural gas system

According to eq. (2.24) and (2.25), several variables are needed to estimate the regional natural gas storage volume $Store_{NG,reg}$, which are the national natural gas storage volume $Store_{NG,nat}$, the national natural gas consumption NG_{nat}, the national final electricity consumption E_{reg}, and the conversion efficiency from natural gas to electricity η_{NG}. The adopted data are listed as below:

Table 3.2: Data related to the natural gas system

Parameter	Value	Unit
$Store_{NG,nat}$	3.14×10^7 [a]	m^3
NG_{nat}	1.65×10^{15} [105]	kJ
E_{reg}	2.34×10^{11} [b]	kJ
η_{NG}	0.68 [c]	-

[a] $Store_{NG,nat}$ is calculated based on the total working capacity of underground storage cavern in the Netherlands (9.3×10^9 m^3 natural gas [62]). The storage conditions are assumed to be 300 bar and 0 °C. [106, 107].

[b] E_{reg} is calculated based on the hourly electricity demand data in Slotermeer provided by Alliander.

[c] η_{NG} is calculated based on the statistical data from CBS [108, 105, 109] which is comparable to 58% from literature [110].

Chapter 4 Results

The following three figures are applicable to the Scenario 1, 2, 3 and 5 which involves micro wind turbines and PV panels. The hourly-based electricity generation by micro wind turbines and PV panels, the hourly electricity demand of Slotermeer, the corresponding electricity surplus from wind and PV power are plotted in Figure 4.1, 4.2 and 4.3 respectively.

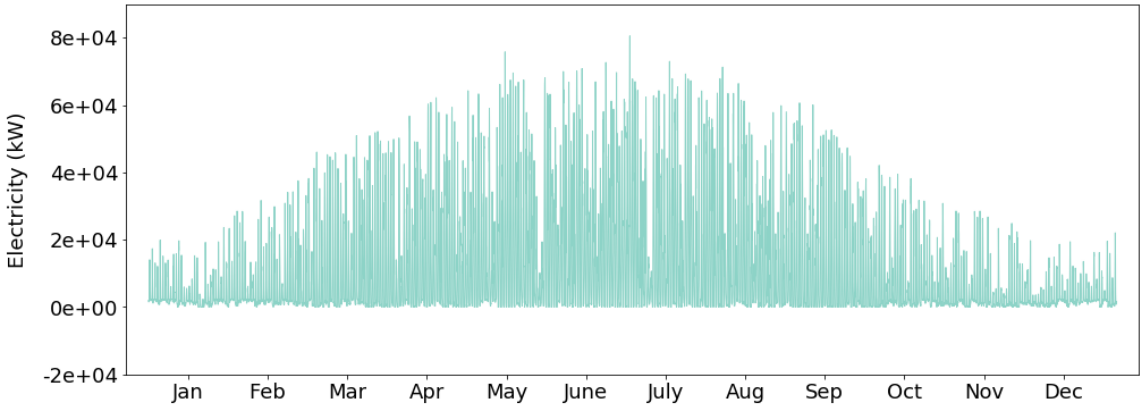

Figure 4.1: Hourly electricity generated by micro wind turbines and PV panels

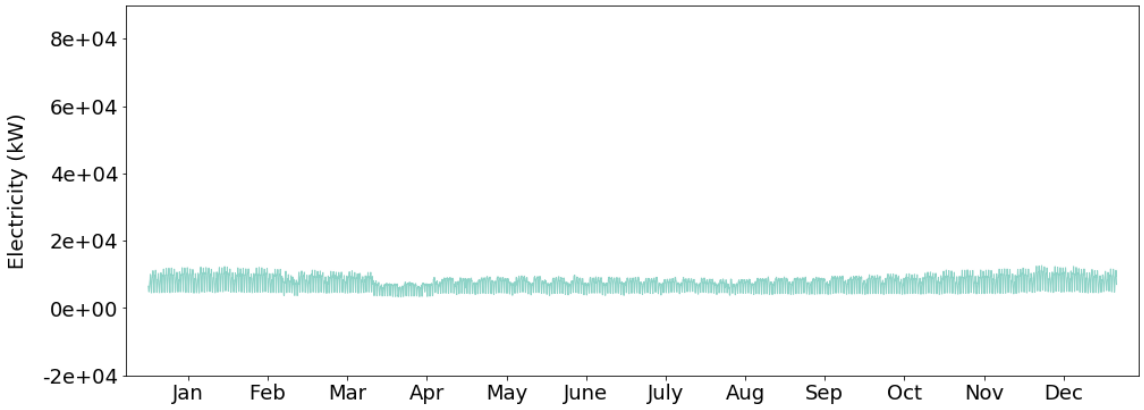

Figure 4.2: Hourly electricity demand

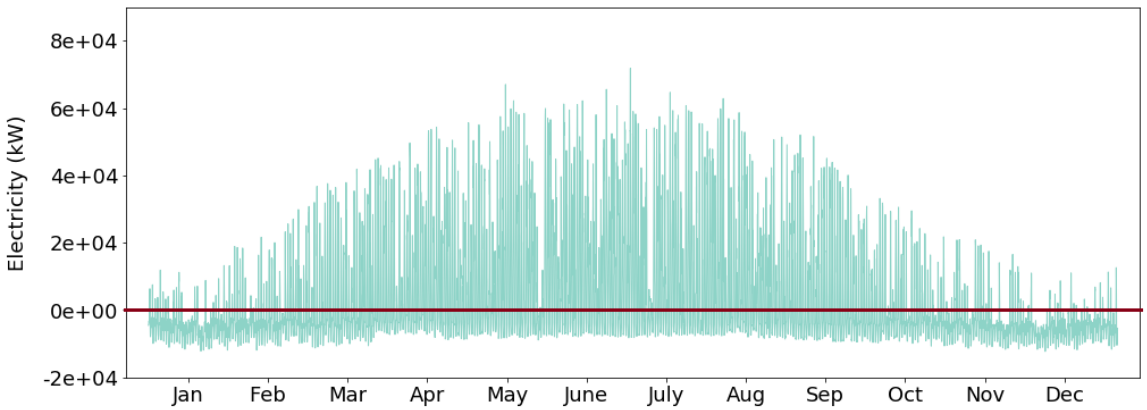

Figure 4.3: Hourly electricity surplus from wind and PV power

Figure 4.1 shows a trend similar to the seasonal change of solar irradiance. In every month there are some hours with no electricity generation. This is due to the lack of solar radiation during night and weak wind. The hourly electricity demand is simulated according to the statistical data (Figure 4.2). The demand in cold seasons are a little higher than that in spring and summer. Figure 4.3 is calculated by the subtraction of Figure 4.1 and 4.2. When the wind/PV-generated power is larger than the demand, the positive surplus occurs, vice versa. It can be observed even in summer when the solar irradiation is intense and the duration time is longer, energy shortage still occurs during night.

4.1 Comparison between HRESs with and without MPC

To verify whether the MPC facilitates the energy management, the performances of HRESs with and without MPC were compared in Scenario 1. The results of comparison including the glucose concentration in feed, hourly H_2 produced via fermentation and hydrogen storage are plotted in the following figures. The design parameters are listed in Table 4.1. The reference control input levels $G_{0,A}$ and $G_{0,B}$ are taken as 0.27 and 27.23 g/L respectively.

4.1.1 Glucose concentration in feed

By applying MPC, the glucose concentration in the feed is manipulated to match the time-variant demand and supply (Figure 4.4). The high level glucose is mainly applied in winter season when the solar and wind power is not sufficient (Figure 4.1). From May on, the glucose is delivered in low concentration just to keep the micro-organisms alive.

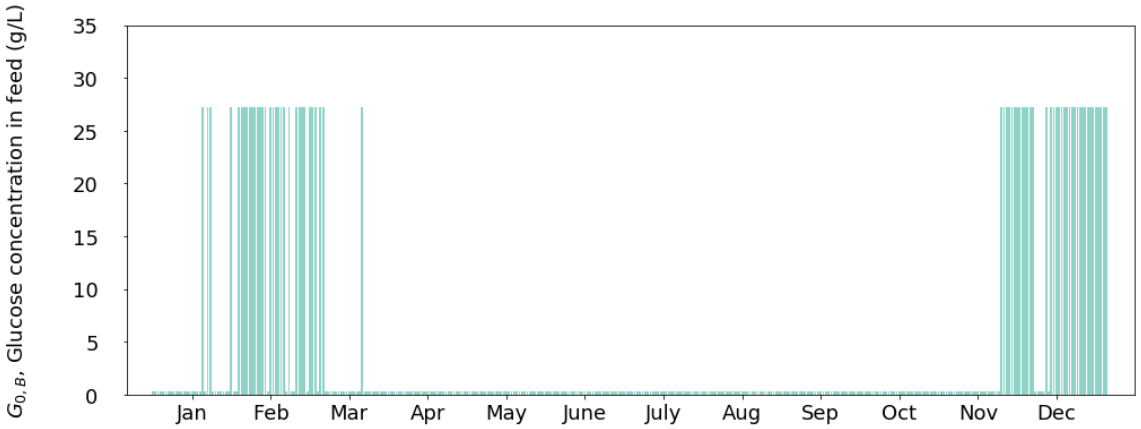

Figure 4.4: Hourly glucose concentration in feed with MPC

According to the results of optimization, the total glucose consumption in 2014 can be determined. For the same configuration of HRES without MPC, the same amount of total glucose consumption was assumed to be distributed evenly over a year (Figure 4.5).

4.1.2 Bio-hydrogen production

Due to the different feeding strategies, the hydrogen produced via fermentation shows two different trends (the detailed dynamics of fermentation can be found in Appendix A). The fermentation system with MPC appears an undulant motion (Figure 4.6). The bio-hydrogen production with steady feeding keeps low, constant production over the year (Figure 4.7).

4.1.3 Hydrogen storage

Since the MPC does not affect the behaviours of electrolyzers and fuel cells, the related responses are not presented here but can be found in Appendix A Figure A.4 - A.9.

Figure 4.8 shows that the hydrogen storage presents a distinct wave of which the trend is a bit delayed than the trend of wind and solar power (Figure 4.1). In the first month the system runs smoothly without high glucose concentration. The reason for low demand in glucose is the initial storage of 40% where it

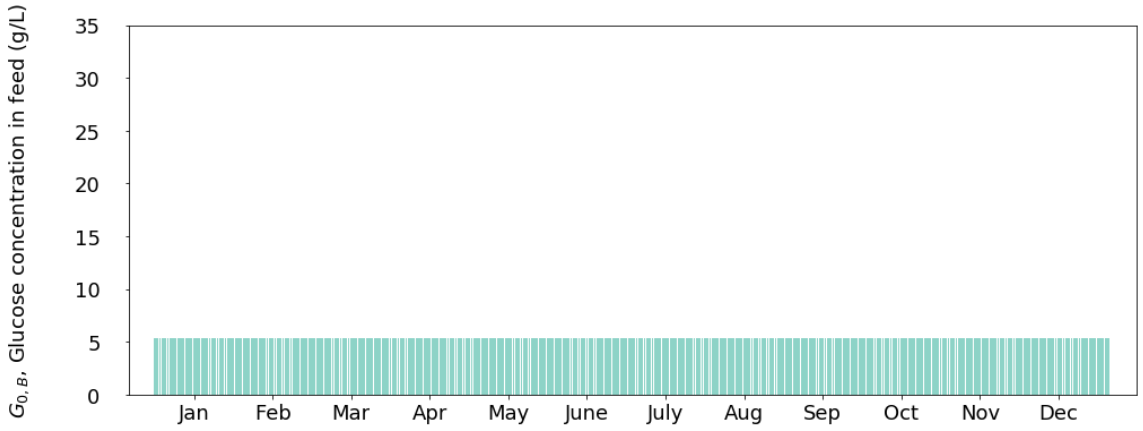

Figure 4.5: Hourly glucose concentration in feed without MPC

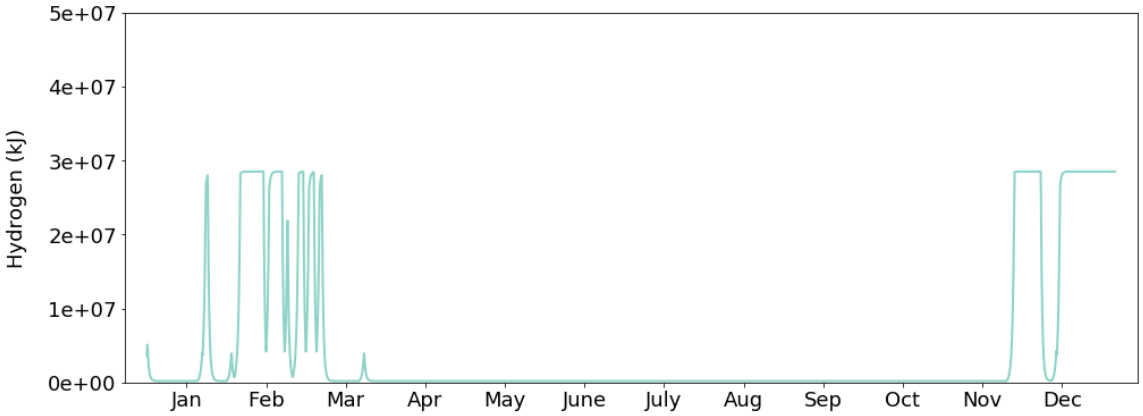

Figure 4.6: Hourly H_2 produced via fermentation with MPC

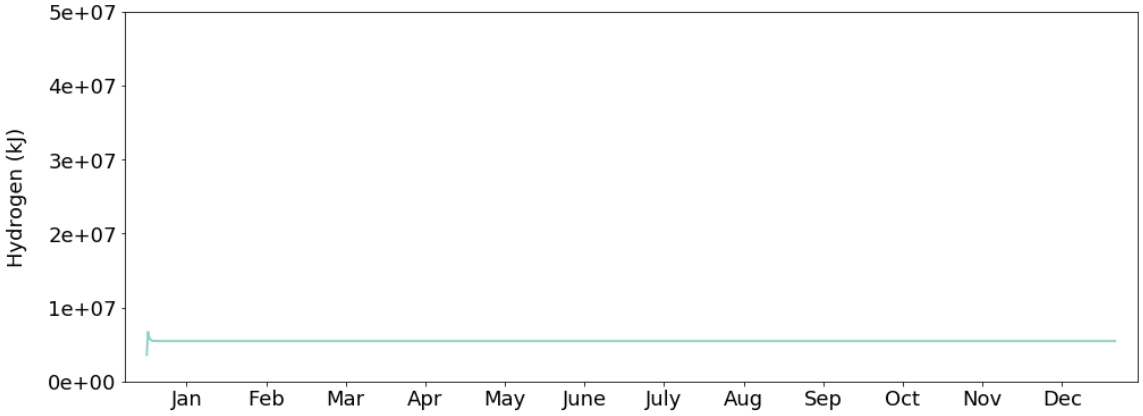

Figure 4.7: Hourly H_2 produced via fermentation without MPC

sustain on. Starting from the beginning of February, the fermentation system is fed with concentrated glucose to cope with the low wind and PV power supply in order to keep the storage above the lower bound. As the solar radiation duration and intensity increases, the power from micro wind turbines and PV cells exceed the electricity demand. The MPC stops providing concentrated glucose and begins to store the extra power from solar irradiation. Until mid-September, the storage reaches a peak value, which means the hourly hydrogen production and consumption are nearly equivalent. Afterwards, due to the decreased wind and PV power in winter and the constraint on the storage level at the end of the year (represented by the penalty term in the cost function, see Section 2.5), concentrated glucose is

delivered.

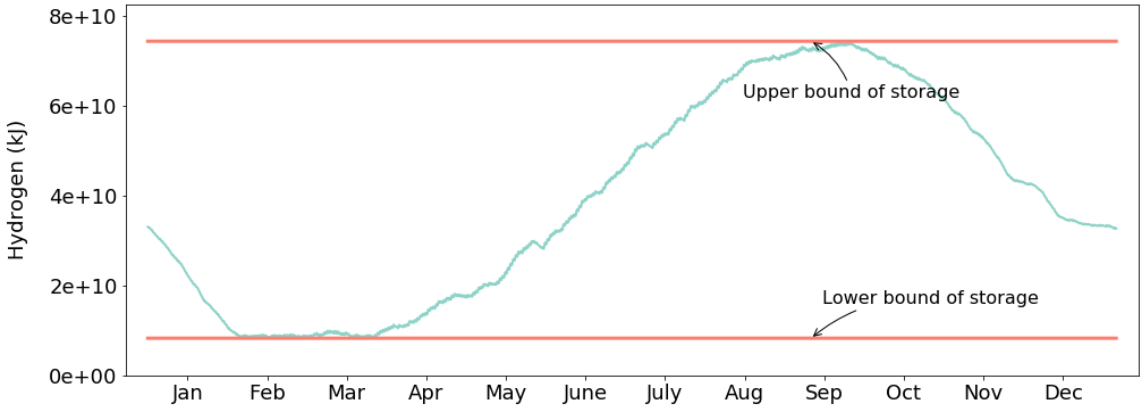

Figure 4.8: Hydrogen storage with MPC

In contrast, the constant bio-hydrogen supply without MPC ignores the future behaviours of wind and PV power. The amount of stored hydrogen exceeds the capacity of storage tank (Figure 4.9). This is because without MPC the bio-energy system cannot be complementary to the fluctuating renewable energy but simply an addition.

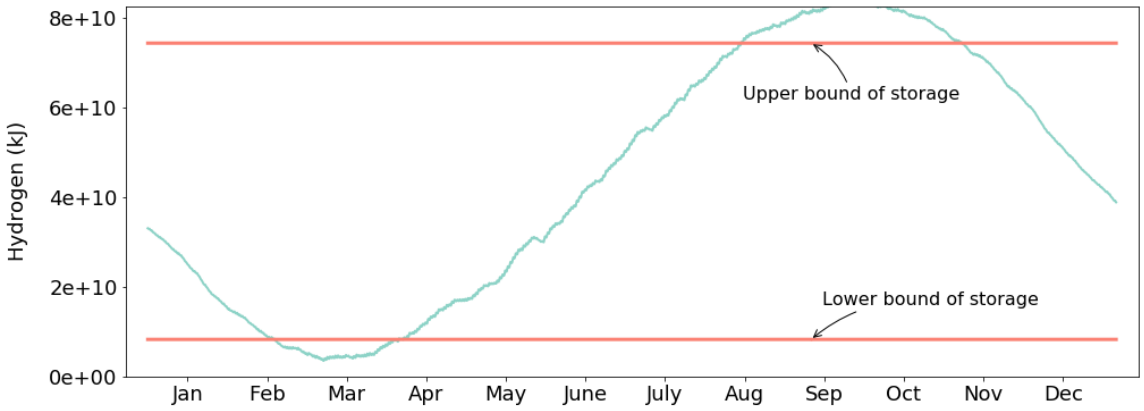

Figure 4.9: Hydrogen storage without MPC

It can be imagined that a HRES without MPC would work when the storage system is large enough. Yet any increases in size of such an enormous energy system for a city district will be a significant waste in terms of space, costs, as well as resources. Moreover, a HRES without MPC is not capable of dealing multiple constraints such as lower/upper bound of storage and disturbances automatically.

4.2 Comparison among different configurations of HRES

Three possible configurations of HRES presented in Section 2.2.1 have their own merits and weaknesses. To make an intuitive comparison, Scenario 1 is taken as a reference, and all the parameters in Scenario 1 are represented by factor '1'. Then the parameters and outputs of other two scenarios are divided by the corresponding values in Scenario 1 to obtain the relative factors. Thus, the size and performance of three HRESs can be compared relatively. The result is presented in Figure 4.10. See Appendix A for detailed dynamics and Appendix B for complete simulation results of each scenario. The design parameters are listed in Table 4.1. The reference control input levels $G_{0,A}$ and $G_{0,B}$ are taken as 0.27 and 27.23 g/L respectively.

Since the electricity demand is fulfilled by wind, PV power and fuel cells in case of shortage, the capacity of fuel cells are the same for three scenarios. Compared to the other two scenarios, the biggest advan-

Table 4.1: Design parameters of three HRESs

Parameter	Description (unit)	Scenario 1	Scenario 2	Scenario 3
$Cap_{storage}$	Hydrogen storage capacity (kJ)	8.26×10^{10}	1.20×10^{10}	1.50×10^{10}
Cap_{ferm}	Fermentation tank capacity (L)	2.40×10^{6}	3.40×10^{6}	3.10×10^{6}
$L_{storage,LB}$	Lower bound of storage level (%)		10	
$L_{storage,UB}$	Upper bound of storage level (%)		90	
$L_{storage,in}$	Initial storage level (%)	40	80	80

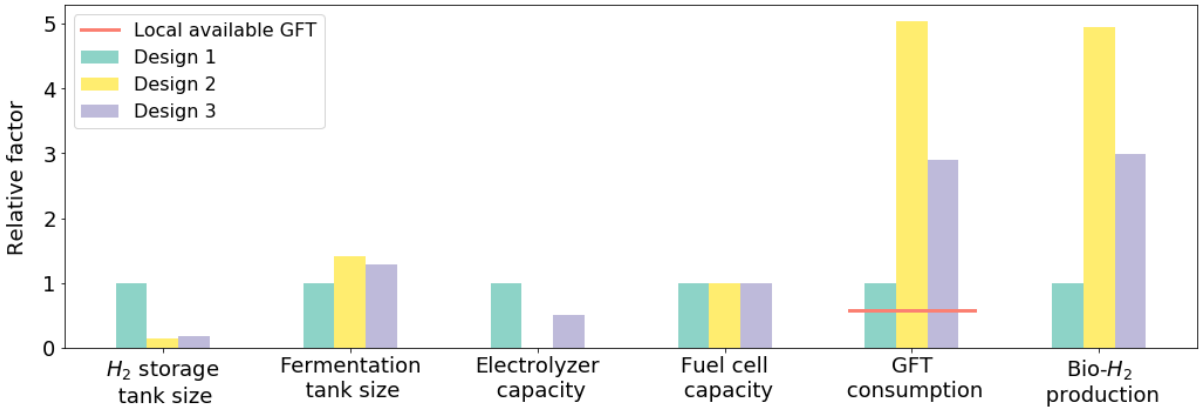

Figure 4.10: Relative comparison among Scenario 1 , 2 & 3

tage of Scenario 2 is no need for electrolyzers since PV and wind power are not converted into hydrogen for storage. However, the disadvantage is the requirement for a large fermentation system as well as a large amount of substrates. As for Scenario 3, the capacity of electrolyzers are reduced by half. The increase of fermentation tank is approximately half of the difference between fermentation tank sizes in Scenario 1 and 2. The GFT and bio-hydrogen production have the similar trends. Although only half of the excess wind and PV energy is delivered into storage system, the size of hydrogen storage tank is significantly reduced. This implies the inflow and outflow of hydrogen tank is much better balanced than those in Scenario 1, which means the storage tank is utilized more efficiently.

However, in all three scenarios, the GFT wastes produced locally cannot totally cover the GFT consumption. Thus, other biomass sources such as wood chips and forestry residues, or importing GFT wastes from other regions should be considered as supplements.

4.3 Normalized control input sensitivity analysis

As explained in Section 2.6, normalized sensitivity analysis of $G_{0,B}$ was performed for three HRES scenarios. By changing the value of $G_{0,B}$, the impact on system outcomes can be determined. The design parameters are listed in Table 4.1. The control input levels (g/L) $G_{0,A}$ and $G_{0,B}$ are presented in Table 4.2.

4.3.1 Scenario 1

The responses of five system outcomes are plotted against $G_{0,B}$ to evaluate the performance of HRESs.

As shown in Figure 4.11, the zoom-in responses of operating cost, bio-H_2 production, ending storage level apparently have linear relations. The different yearly bio-H_2 production leads to the difference in the ending storage level. Since the design parameters and system disturbances are the same for

Table 4.2: Control parameters of three HRESs

Control input levels	**Scenario 1 , 2 & 3**						
$G_{0,A}$ (g/L)	0.27						
$G_{0,B}$ (g/L)	21.78	23.15	24.51	25.87	27.23	28.59	29.95

each simulation, the changes in ending level is proportional to that in bio-hydrogen production. The reason that the changes in operating cost is also linearly related to bio-hydrogen production is because the change in operating cost is coupled with the hydrogen production via fermentation. The detailed explanation can be found in section 2.4.1. As for GFT consumption whose curve is a little different from other three mentioned above, it is because the hydrogen yield slightly varies with different concentration of glucose in-feeds.

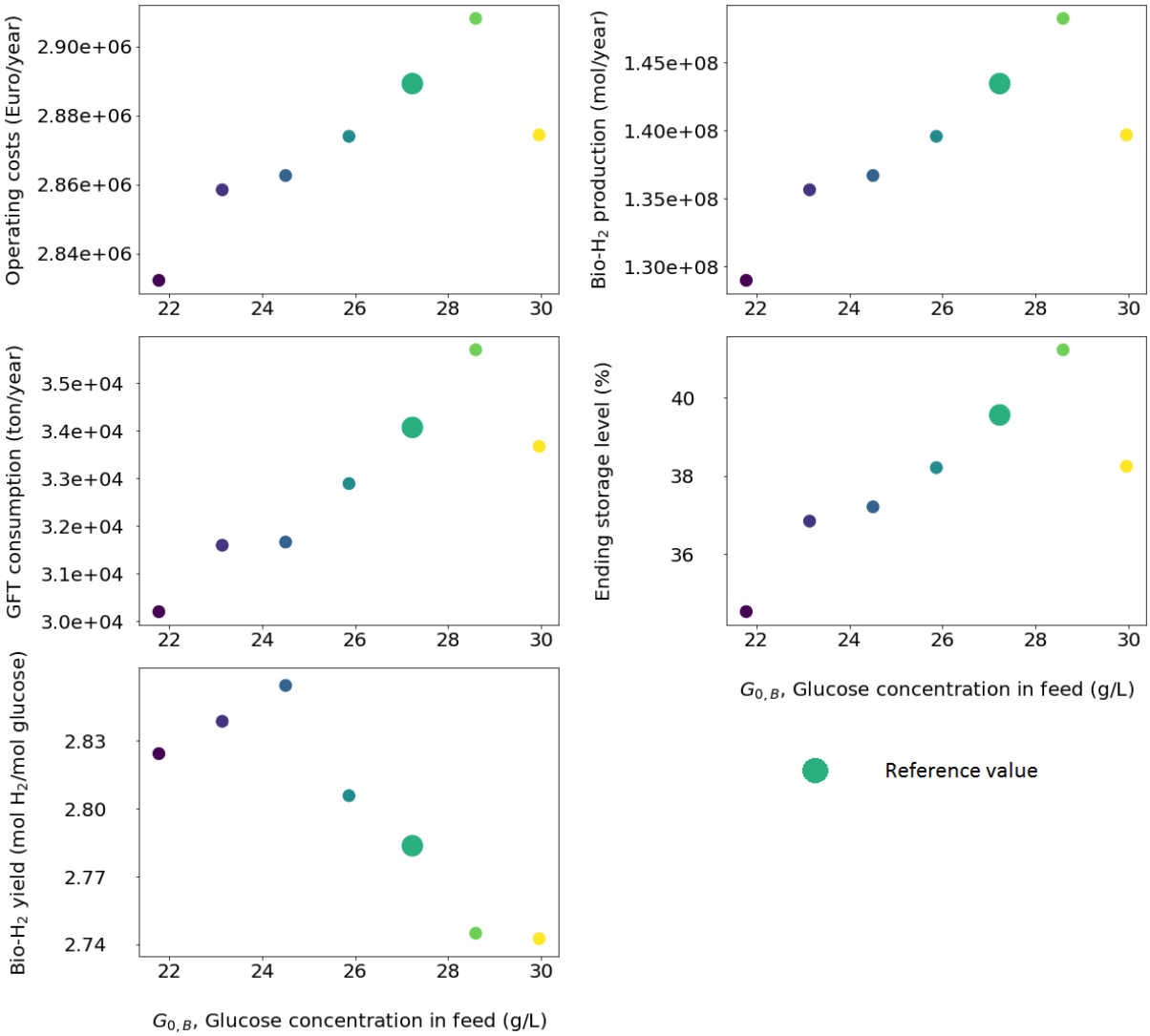

Figure 4.11: System responses with different $G_{0,B}$ for Scenario 1

As the set-point for ending level is a soft constraint, it is allowed for the ending level to vary within a reasonable range. The results with different $G_{0,B}$ are all acceptable. This ensures the system with an appropriate initial state for next year.

According to the result of normalized sensitivity analysis (Figure 4.12), the GFT consumption have the most sensitivity to $G_{0,B}$ which makes sense, because the inflow concentration directly links to the total substrate consumption when the flow rate is fixed. Since the Bio-H_2 yield is less sensitive, the bio-H_2 production has a similar result as GFT consumption does. Although the changes of operating cost is caused by different hydrogen production via fermentation, the proportion of Bio-hydrogen related cost is low in total operating cost, thus the operating costs is the least sensitive term. As a whole, when the high level of glucose concentration in the feed $G_{0,B}$ is between 24 and 25 g/L the system under Scenario 1 is robust because the changes in $G_{0,B}$ do not have significant effects on system performance.

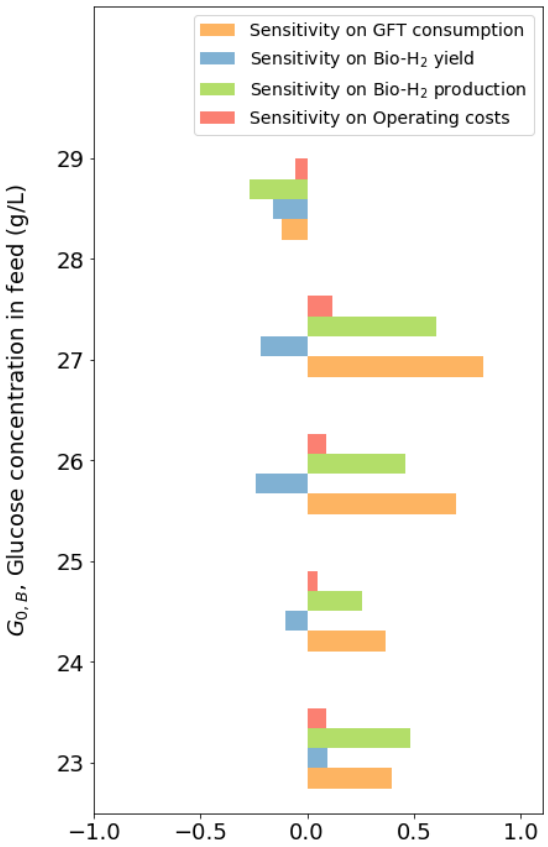

Figure 4.12: Normalized sensitivity of $G_{0,B}$ on system outcomes for Scenario 1

4.3.2 Scenario 2

In Scenario 2, an adjustment of initial level is made to fit the different configuration. When $G_{0,B}$ is above 24 g/L, the ending level is close to 80% which is the initial storage level (Figure 4.13). Apart from this range, the successful running for next round might be endangered. The curve of GFT consumption appears more distinct from others in Scenario 2, which is partially because of bigger changes in hydrogen yield. Moreover, the fermentation system in Scenario 2 is much larger than that in Scenario 1. Therefore, a little change in yield makes big difference in the consumption of substrate.

The normalized sensitivities of system outcomes for Scenario 2 are quite different from that of Scenario 1. The significance of fermentation system in Scenario 2 has been further demonstrated. Since the $G_{0,B}$ below 24 g/L might endanger the reliability of the system, the first data point in Figure 4.14 is considered invalid. As shown in Figure 4.14, bio-H_2 yield becomes the most sensitive term together with GFT consumption. Apparently the positive and negative sensitivities of these two cancelled the effect on Bio-H_2 production. Furthermore, the hydrogen yield decreases more quickly as the $G_{0,B}$ increases.

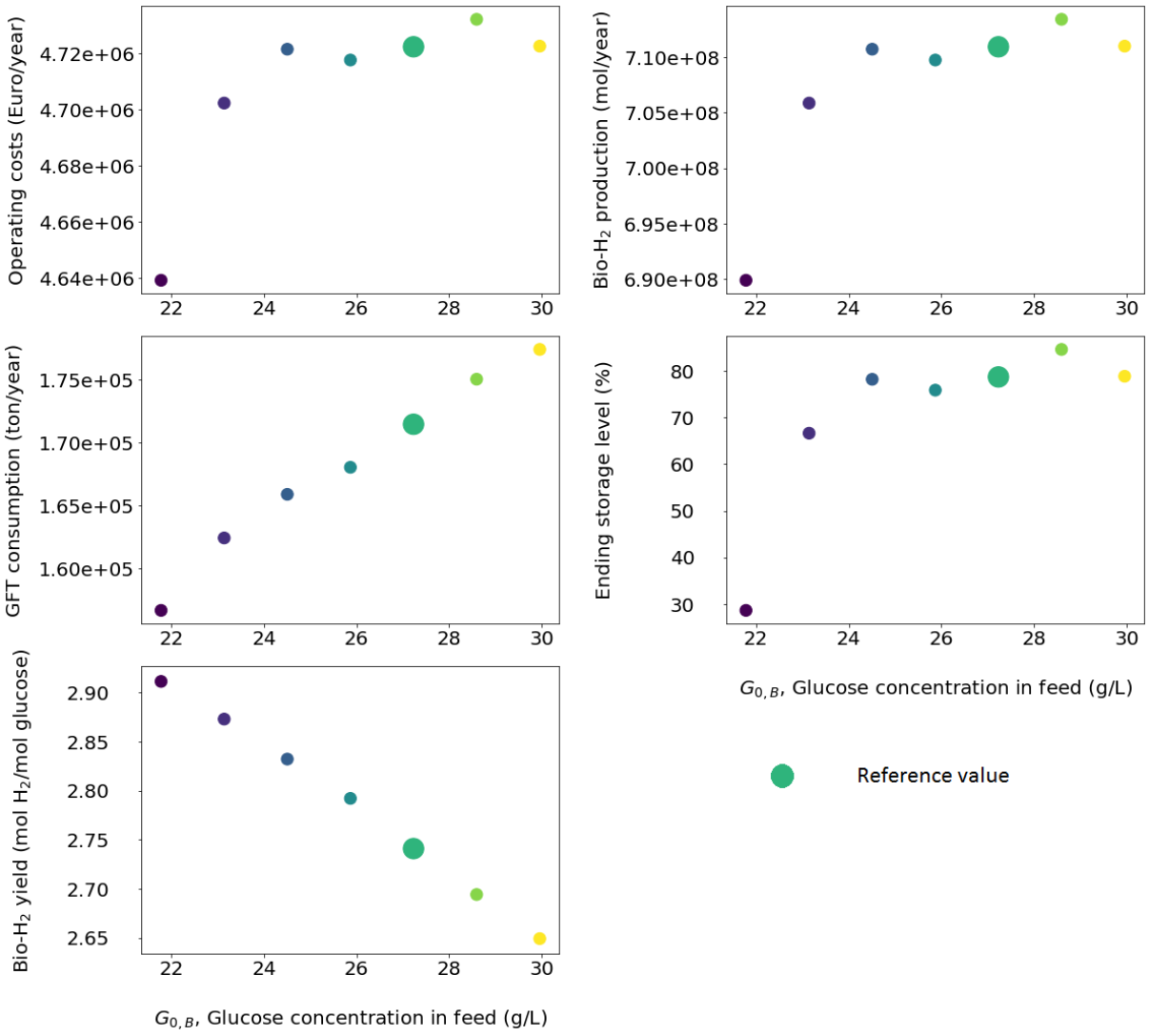

Figure 4.13: System responses with different $G_{0,B}$ for Scenario 2

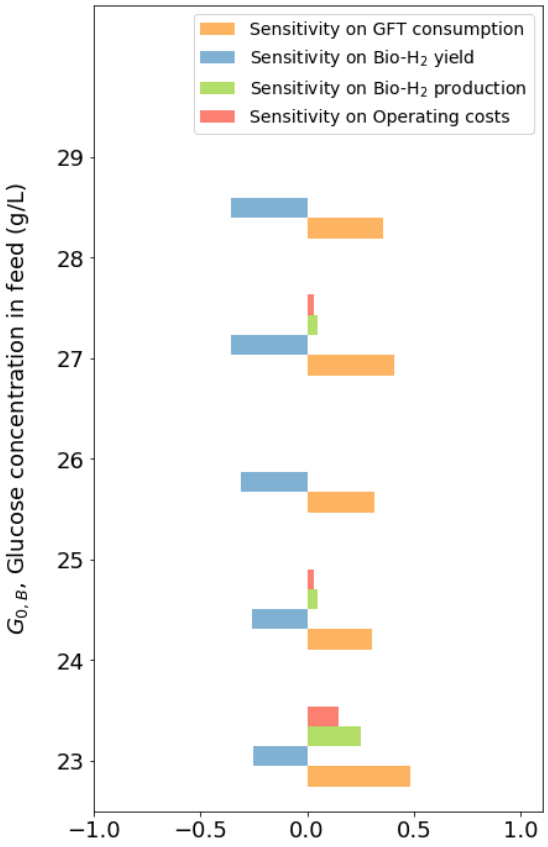

Figure 4.14: Normalized sensitivity of $G_{0,B}$ on system outcomes for Scenario 2

4.3.3 Scenario 3

As an intermediate solution, the results of Scenario 3 can be regarded as the combination of the previous two except for the ending level. The initial level of the feasible solution for Scenario 3 is 80% which is the same as the Scenario 2. A smaller fermentation system with glucose concentration below 26 g/L cannot fulfil the soft constraint on ending level (Figure 4.15).

Considering the reliability, the first two data points are not taken into account in the following discussion (Figure 4.16). From 26 to 29 g/L $G_{0,B}$, the sensitivities go through a transition from Scenario 1 to Scenario 2. This can be interpreted as that when $G_{0,B}$ is low, the H_2 yield is of less importance; as $G_{0,B}$ increases, the HRES becomes more dependent on the efficiency of fermentation system.

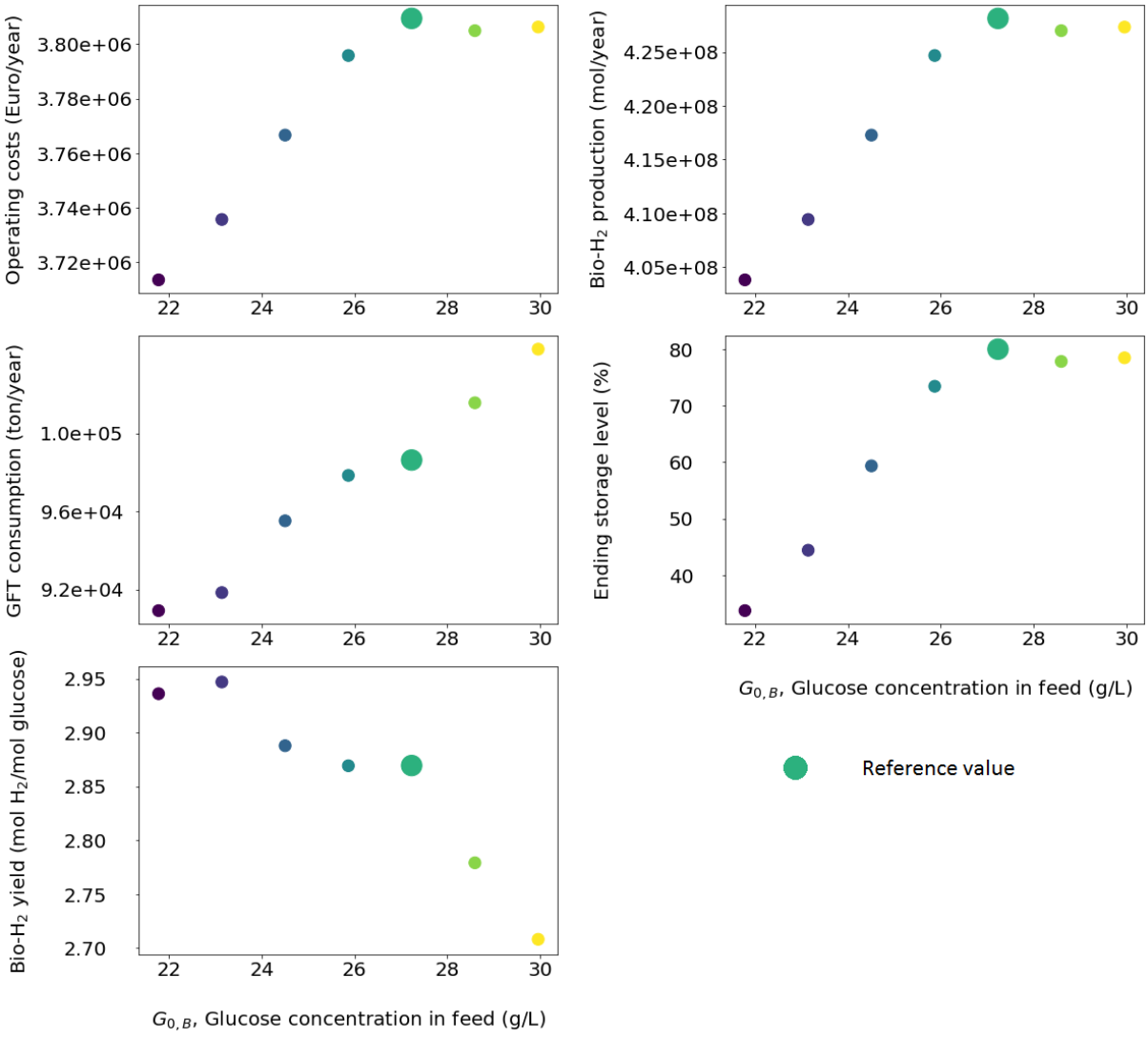

Figure 4.15: System responses with different $G_{0,B}$ for Scenario 3

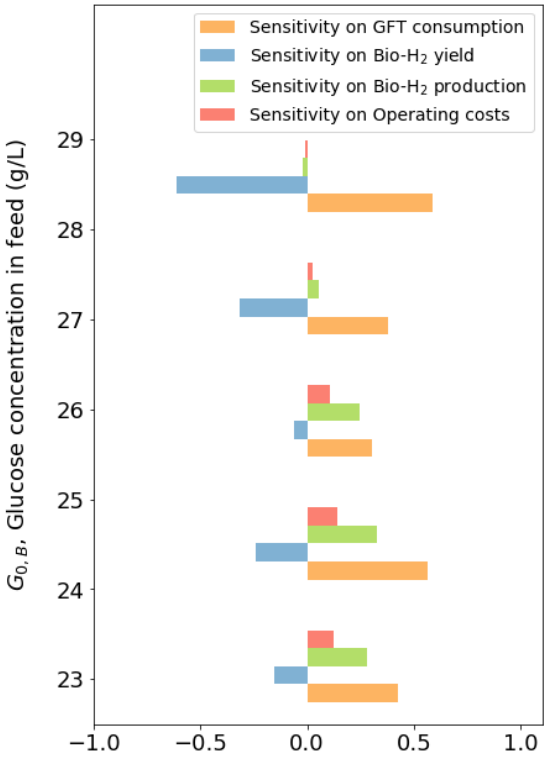

Figure 4.16: Normalized sensitivity of $G_{0,B}$ on system outcomes for Scenario 3

4.4 Natural gas system

4.4.1 Scenario 4

The baseline scenario is a system entirely powered by natural gas. Based on the eq.(2.24) & (2.25) and data from Table 3.2, the yearly natural gas consumption NG_{reg} and the natural gas storage volume in Slotermeer can be roughly estimated as 3.44 $\times$ 10^{11} kJ and 6,550 m^3 respectively.

4.4.2 Scenario 5

Scenario 5 is similar to Scenario 3 in which the fermentation system is substituted by a natural gas system. The simulation result of natural gas system is plotted in Figure 4.17.

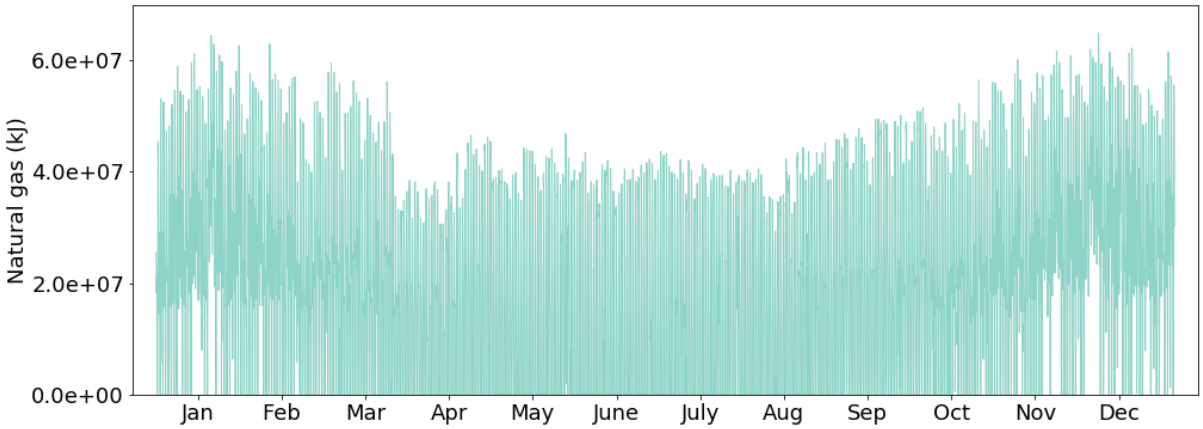

Figure 4.17: Natural gas consumption for Scenario 5

The yearly natural gas consumption NG_{reg} for Scenario 5 is 1.73 $\times$ 10^{11} kJ. According to eq.(2.25), and the natural gas storage volume is calculated as 3,310 m^3.

4.5 HRES vs Natural gas system

Based on the results obtained in Section 4.2 and 4.4, a comparison between the storage sizes of stand-alone HRES and natural gas system can be made. The result is shown in Figure 4.18. In respect of storage size, Scenario 2 and 3 have major advantage over natural gas scenarios.

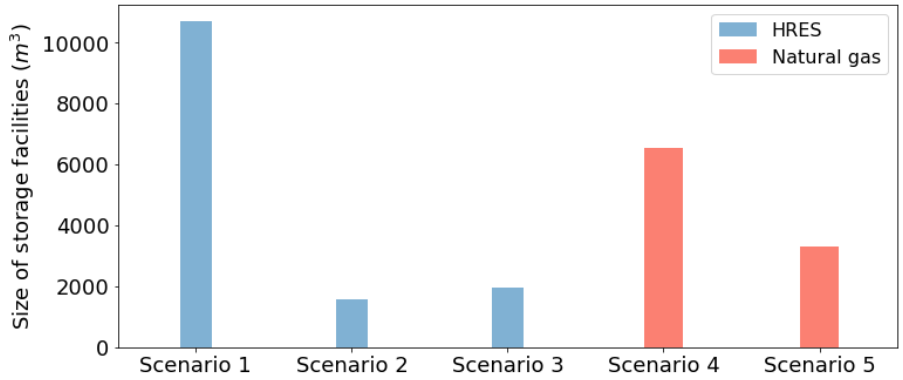

Figure 4.18: Comparison of storage sizes between HRESs and Natural gas systems

Chapter 5 General Discussion

During the study, three possible configuration of HRES were proposed and their merits and shortcomings were compared. The positive effect of model predictive control on energy management was validated by performing a case study in Slotermeer, Amsterdam. A normalized sensitivity analysis was performed to investigate the effects of the glucose concentration in the feed stream on the HRES performance.

However, due to the time and data limitations, the economic feasibility of the HRESs were not studied in depth. A simple comparison about the sizes of storage systems between natural gas system and HRES was made. As one of the most important energy carriers, natural gas adopts a centralized management strategy. Natural gas is transported through pipelines which connect its storage facilities crossing several countries. In the study only underground storage is taken as a storage volume, yet in reality the transport pipelines might also contribute to the storage. It is difficult to estimate the total size and costs of a stand-alone system for one district. For a conceptual design, most of the components such as hydrogen storage unit and electrolyzers are in large size. Usually the large equipment are custom-made which makes it difficult to find the related economic parameters.

As explained in Section 4.2, the preliminary study on the compromising solution, Scenario 2, shows an efficient usage of the storage system and less dependence on fermentation. A pre-defined ratio of 0.5 to 0.5 is used to split the energy stream. However, more flexibilities should be introduced to regulate the energy flow.

Since the focus of this study is the combination of hydrogen energy and fluctuated solar and wind power, the anaerobic fermentation process was simplified to serve the goal. In fact, the hydrogen production via fermentation is sometimes coupled with the formation of methane which is the dominant energy source in the Netherlands [111, 61]. In the proposed HRES, the products from anaerobic fermentation are assumed to be separated and purified. The purified bio-methane then can be merged into the local natural gas pipelines or delivered to households. The fermentation system needs to be operated at about 35 $^{\circ}C$. The heat generated by fermentation process is not enough for biomass production, thus external energy is required. This part of energy consumption is not included as an energy stream in the HRES, but simply as an operating cost. Similarly, dynamics inside electrolyzers and fuel cells are simplified to efficiency factors. And the AC/DC conversion which is beyond the subject is also included in the study.

In Scenario 2, 3 and 5, the excess electricity was exported directly to the power grid. However in reality, the import of a large amount of electric current in a short time could cause serious disturbances in the grid. This issue needs to be addressed in practice.

Chapter 6 Conclusions

In this study, three possible configurations of HRES system involving anaerobic fermentation and hydrogen storage system are proposed. The major energy source of the HRES in Scenario 1 are wind and PV power. The bio-H_2 works as a complement to cope with the electricity shortage caused by seasonal change. Although the fermentation system in Scenario 1 is smaller than that in other two scenarios, it is in low use in 3/4 time of a year. Furthermore the large hydrogen storage system is used mainly to deal with the seasonal energy fluctuations. Scenario 2 holds two advantages which are the avoiding of electrolyzers and small size of storage tank. The HRES is highly dependent on bio-fermentation system which leads to a bigger fermenter and large GFT wastes consumption which is far beyond what Slotermeer can provide. Therefore, external biomass source needs to be included such as lignocellulosic residues from forestry, agricultural and algae residues, etc [45]. The successful running of the HRES in Scenario 2 better incorporates the production of bio-methane to balance the material costs. The Scenario 3, a compromising scheme between Scenario 1 and 2, presents a more flexible solution. Compared to Scenario 2, a small increase in the size of storage tank brings significant reduction in GFT consumption. The better utilization of storage tank shows that the original fluctuated power provided by wind and solar generator is excess for Slotermeer. The stable energy source which is bio-hydrogen plays an important role in the system.

The model predictive controller provides reliable predictions about system behaviours and considering various constraints. It turns the complex control problem into a minimization of cost function. As shown in Section 4.1.3, by applying MPC, the size of storage tank is successfully reduced. It is worth noting that the initial state is absolutely important for a system with highly fluctuated disturbances. In the three scenarios, the initial tank level is a determined operating parameter.

The glucose concentration in feed has been demonstrated to have distinct influences on GFT consumption, bio-H_2 yield and bio-H_2 production. Among all three scenarios, GFT consumption is the most sensitive parameter to the glucose concentration. For HRES with small fermentation system such as Scenario 1, bio-H_2 production is positively sensitive which is related to the GFT consumption. However for HRES with larger fermentation system, as in Scenario 2 and 3, the bio-H_2 yield has an apparently negative sensitivity. The negative sensitivity of bio-H_2 yield and the positive sensitivity of GFT consumption cancel the effect of glucose concentration in feed on the bio-H_2 production. Overall, the system performance is robust when the glucose concentration in feed is in range of 25 to 28 g/L. Apart from this range, the feasibility of subsequent running for years will be endangered.

To sum up the study, the three HRESs possess respective merits which suit different circumstances. However in the case of Slotermeer, the optimal HRES configuration is Scenario 3 in terms of performance and utilization of equipment. Model predictive controller fully utilizes the historical data, weather forecast, mathematical models to predict system behaviour and manage energy streams. In general, the HRESs are more robust when the high-level of glucose concentration in the feed is between 25 to 28 g/L.

For future research, two options are suggested. As mentioned before that more flexibilities are possible in Scenario 3. By changing the fixed ratio or more radically, adding another controller to manage the energy stream from PV cells an wind turbines in order to realize the entirely optimal control of the HRES. Another direction is to further investigate the economic aspects of HRESs to find the concrete proof that bio-based HRES is feasible technically and economically as well.

Acknowledgements

I would like to express my gratitude to all those who helped me during the thesis research.

My deepest gratitude first and foremost goes to my supervisors, Dr.Karel Keesmand and MSc.Yu Jiang, for their constant encouragement and patient guidance. This thesis would not have been possible without their contributions.

Second, I would like to thank my thesis-ring group for providing me with valuable suggestions on scientific writings.

Finally I would like to thank Biobased Chemistry & Technology (BCT) group of Wageningen University & Research for providing quality resource to support this interesting case.

References

[1] IEA, "Key world energy statistics 2016," in *Key world energy statistics 2016*, 2016.

[2] L. Pérez-Lombard, J. Ortiz, and C. Pout, "A review on buildings energy consumption information," *Energy and Buildings*, vol. 40, no. 3, pp. 394–398, 2008.

[3] Eurostat, "Final energy consumption by sector 2014," 2014. `http://ec.europa.eu/eurostat/tgm/table.do?tab=table&plugin=1&language=en&pcode=tsdpc320`.

[4] M. Santamouris, N. Papanikolaou, I. Livada, I. Koronakis, C. Georgakis, A. Argiriou, and D. Assimakopoulos, "On the impact of urban climate on the energy consumption of buildings," *Solar energy*, vol. 70, no. 3, pp. 201–216, 2001.

[5] M. Deshmukh and S. Deshmukh, "Modeling of hybrid renewable energy systems," *Renewable and Sustainable Energy Reviews*, vol. 12, no. 1, pp. 235–249, 2008.

[6] A. González, J.-R. Riba, and A. Rius, "Optimal sizing of a hybrid grid-connected photovoltaic–wind–biomass power system," *Sustainability*, vol. 7, no. 9, pp. 12787–12806, 2015.

[7] O. Erdinc and M. Uzunoglu, "Optimum design of hybrid renewable energy systems: Overview of different approaches," *Renewable and Sustainable Energy Reviews*, vol. 16, no. 3, pp. 1412 – 1425, 2012.

[8] A. S. Al Busaidi, "A review of optimum sizing techniques for off-grid hybrid PV-wind renewable energy systems," *International Journal of Students' Research in Technology & Management*, vol. 2, no. 3, pp. 93–102, 2015.

[9] R. Siddaiah and R. Saini, "A review on planning, configurations, modeling and optimization techniques of hybrid renewable energy systems for off grid applications," *Renewable and Sustainable Energy Reviews*, vol. 58, pp. 376–396, 2016.

[10] P. Nema, R. Nema, and S. Rangnekar, "A current and future state of art development of hybrid energy system using wind and PV-solar: A review," *Renewable and Sustainable Energy Reviews*, vol. 13, no. 8, pp. 2096–2103, 2009.

[11] H. Yang, L. Lu, and J. Burnett, "Weather data and probability analysis of hybrid photovoltaic–wind power generation systems in Hong Kong," *Renewable Energy*, vol. 28, no. 11, pp. 1813 – 1824, 2003.

[12] R. Karki and R. Billinton, "Reliability/cost implications of PV and wind energy utilization in small isolated power systems," *IEEE Transactions on Energy Conversion*, vol. 16, pp. 368–373, Dec 2001.

[13] J. Ding, J. Buckeridge, *et al.*, "Design considerations for a sustainable hybrid energy system," *Transactions of the Institution of Professional Engineers New Zealand: Electrical/Mechanical/Chemical Engineering Section*, vol. 27, no. 1, p. 1, 2000.

[14] S. Jain and V. Agarwal, "An integrated hybrid power supply for distributed generation applications fed by nonconventional energy sources," *IEEE Transactions on Energy Conversion*, vol. 23, pp. 622–631, June 2008.

[15] A. Bhave, "Hybrid solar–wind domestic power generating system—a case study," *Renewable Energy*, vol. 17, no. 3, pp. 355 – 358, 1999.

[16] M. Elhadidy and S. Shaahid, "Parametric study of hybrid (wind+ solar+ diesel) power generating systems," *Renewable Energy*, vol. 21, no. 2, pp. 129–139, 2000.

[17] J. G. Vera, "Options for rural electrification in Mexico," *IEEE Transactions on Energy Conversion*,

vol. 7, no. 3, pp. 426–433, 1992.

[18] B. Wichert, "PV-diesel hybrid energy systems for remote area power generation—a review of current practice and future developments," *Renewable and Sustainable Energy Reviews*, vol. 1, no. 3, pp. 209–228, 1997.

[19] P. Bajpai and V. Dash, "Hybrid renewable energy systems for power generation in stand-alone applications: a review," *Renewable and Sustainable Energy Reviews*, vol. 16, no. 5, pp. 2926–2939, 2012.

[20] R. Ahluwalia and J. Peng, "Automotive hydrogen storage system using cryo-adsorption on activated carbon," *International Journal of Hydrogen Energy*, vol. 34, no. 13, pp. 5476–5487, 2009.

[21] B. Shakya, L. Aye, and P. Musgrave, "Technical feasibility and financial analysis of hybrid wind–photovoltaic system with hydrogen storage for Cooma," *International Journal of Hydrogen Energy*, vol. 30, no. 1, pp. 9–20, 2005.

[22] A. Züttel, A. Borgschulte, and L. Schlapbach, *Hydrogen as a future energy carrier*. John Wiley & Sons, 2011.

[23] C. E. G. P. F. Lau, ed., *Advanced in Hydrogen Energy*. Kluwer Academic Publishers, 2002.

[24] K. Mazloomi and C. Gomes, "Hydrogen as an energy carrier: prospects and challenges," *Renewable and Sustainable Energy Reviews*, vol. 16, no. 5, pp. 3024–3033, 2012.

[25] K. Zeng and D. Zhang, "Recent progress in alkaline water electrolysis for hydrogen production and applications," *Progress in Energy and Combustion Science*, vol. 36, no. 3, pp. 307–326, 2010.

[26] S. O. Jekayinfa and V. Scholz, "Potential availability of energetically usable crop residues in Nigeria," *Energy Sources, Part A: Recovery, Utilization, and Environmental Effects*, vol. 31, no. 8, pp. 687–697, 2009.

[27] S. Ladanai and J. Vinterbäck, "Global potential of sustainable biomass for energy," tech. rep., 2009.

[28] M. Charles, R. Ryan, R. Oloruntoba, T. Heidt, and N. Ryan, "The EU-Africa Energy Partnership: Towards a mutually beneficial renewable transport energy alliance?," *Energy Policy*, vol. 37, no. 12, pp. 5546–5556, 2009.

[29] H. H. Larsen, R. K. Feidenhans'l, and L. Sønderberg Petersen, *Risø energy report 3. Hydrogen and its competitors*. 2004.

[30] D. Thrän, M. Dotzauer, V. Lenz, J. Liebetrau, and A. Ortwein, "Flexible bioenergy supply for balancing fluctuating renewables in the heat and power sector—a review of technologies and concepts," *Energy, Sustainability and Society*, vol. 5, no. 1, p. 35, 2015.

[31] P.-L. Chang, C.-W. Hsu, C.-M. Hsiung, and C.-Y. Lin, "Constructing an innovative bio-hydrogen integrated renewable energy system," *International Journal of Hydrogen Energy*, vol. 38, no. 35, pp. 15660–15669, 2013.

[32] E. Kırtay, "Recent advances in production of hydrogen from biomass," *Energy conversion and management*, vol. 52, no. 4, pp. 1778–1789, 2011.

[33] B. Havva and E. Kırtay, "Hydrogen from biomass–present scenario and future prospects," *International Journal of Hydrogen Energy*, vol. 35, no. 14, pp. 7416–7426, 2010.

[34] A. Patel, N. Maheshwari, P. Vijayan, and R. Sinha, "A study on sulfur-iodine (SI) thermochemical water splitting process for hydrogen production from nuclear heat," in *Sixteenth annual conference of Indian Nuclear Society: science behind nuclear technology*, 2005.

[35] S. M. Swami, V. Chaudhari, D.-S. Kim, S. J. Sim, and M. A. Abraham, "Production of hydrogen from glucose as a biomass simulant: integrated biological and thermochemical approach," *Industrial*

& Engineering Chemistry Research, vol. 47, no. 10, pp. 3645–3651, 2008.

[36] D. Das and T. Veziroğlu, "Hydrogen production by biological processes: a survey of literature," *International Journal of Hydrogen Energy*, vol. 26, no. 1, pp. 13 – 28, 2001.

[37] P.-Y. Lin, L.-M. Whang, Y.-R. Wu, W.-J. Ren, C.-J. Hsiao, S.-L. Li, and J.-S. Chang, "Biological hydrogen production of the genus $clostridium$: metabolic study and mathematical model simulation," *International Journal of Hydrogen Energy*, vol. 32, no. 12, pp. 1728–1735, 2007.

[38] X. Zhi, H. Yang, S. Berthold, C. Doetsch, and J. Shen, "Potential improvement to a citric wastewater treatment plant using bio-hydrogen and a hybrid energy system," *Journal of Power Sources*, vol. 195, no. 19, pp. 6945 – 6953, 2010.

[39] A. Pérez-Navarro, D. Alfonso, C. Álvarez, F. Ibáñez, C. Sánchez, and I. Segura, "Hybrid biomass-wind power plant for reliable energy generation," *Renewable Energy*, vol. 35, no. 7, pp. 1436 – 1443, 2010. Special Section: IST National Conference 2009.

[40] P. Balamurugan, S. Kumaravel, and S. Ashok, "Optimal operation of biomass gasifier based hybrid energy system," *ISRN Renewable Energy*, vol. 2011, 2011.

[41] R. Toonssen, S. Sollai, P. Aravind, N. Woudstra, and A. H. Verkooijen, "Alternative system designs of biomass gasification SOFC/GT hybrid systems," *International Journal of Hydrogen Energy*, vol. 36, no. 16, pp. 10414 – 10425, 2011. European Fuel Cell 2009.

[42] G. Liu, M. G. Rasul, M. T. O. Amanullah, and M. M. K. Khan, "Feasibility study of stand-alone PV-wind-biomass hybrid energy system in Australia," in *2011 Asia-Pacific Power and Energy Engineering Conference*, pp. 1–6, March 2011.

[43] N. Ren, J. Li, B. Li, Y. Wang, and S. Liu, "Biohydrogen production from molasses by anaerobic fermentation with a pilot-scale bioreactor system," *International Journal of Hydrogen Energy*, vol. 31, no. 15, pp. 2147 – 2157, 2006.

[44] J.-J. Lay, Y.-J. Lee, and T. Noike, "Feasibility of biological hydrogen production from organic fraction of municipal solid waste," *Water research*, vol. 33, no. 11, pp. 2579–2586, 1999.

[45] M. Ni, M. K. Leung, K. Sumathy, and D. Y. Leung, "Potential of renewable hydrogen production for energy supply in Hong Kong," *International Journal of Hydrogen Energy*, vol. 31, no. 10, pp. 1401 – 1412, 2006.

[46] M. Killian and M. Kozek, "Ten questions concerning model predictive control for energy efficient buildings," *Building and Environment*, vol. 105, pp. 403–412, 2016.

[47] J. L. Bernal-Agustín and R. Dufo-Lopez, "Simulation and optimization of stand-alone hybrid renewable energy systems," *Renewable and Sustainable Energy Reviews*, vol. 13, no. 8, pp. 2111–2118, 2009.

[48] M. Uzunoglu, O. Onar, and M. Alam, "Modeling, control and simulation of a PV/FC/UC based hybrid power generation system for stand-alone applications," *Renewable Energy*, vol. 34, no. 3, pp. 509–520, 2009.

[49] A. Bilodeau and K. Agbossou, "Control analysis of renewable energy system with hydrogen storage for residential applications," *Journal of power sources*, vol. 162, no. 2, pp. 757–764, 2006.

[50] M. Athari and M. Ardehali, "Operational performance of energy storage as function of electricity prices for on-grid hybrid renewable energy system by optimized fuzzy logic controller," *Renewable Energy*, vol. 85, pp. 890–902, 2016.

[51] P. García, J. P. Torreglosa, L. M. Fernández, and F. Jurado, "Optimal energy management system for stand-alone wind turbine/photovoltaic/hydrogen/battery hybrid system with supervisory control based on fuzzy logic," *International Journal of Hydrogen Energy*, vol. 38, no. 33, pp. 14146–14158,

2013.

[52] P. Joshi and J. Valasek, "Direct comparison of neural network, fuzzy logic and model predictive variable structure vortex flow controllers," in *Guidance, Navigation, and Control Conference and Exhibit*, p. 4279, 1999.

[53] S. Vosen and J. Keller, "Hybrid energy storage systems for stand-alone electric power systems: optimization of system performance and cost through control strategies," *International Journal of Hydrogen Energy*, vol. 24, no. 12, pp. 1139 – 1156, 1999.

[54] B. Bhandari, K.-T. Lee, G.-Y. Lee, Y.-M. Cho, and S.-H. Ahn, "Optimization of hybrid renewable energy power systems: A review," *International Journal of Precision Engineering and Manufacturing-Green Technology*, vol. 2, no. 1, pp. 99–112, 2015.

[55] R. Viral and D. Khatod, "Optimal planning of distributed generation systems in distribution system: A review," *Renewable and Sustainable Energy Reviews*, vol. 16, no. 7, pp. 5146–5165, 2012.

[56] E. Koutroulis and D. Kolokotsa, "Design optimization of desalination systems power-supplied by PV and W/G energy sources," *Desalination*, vol. 258, no. 1–3, pp. 171 – 181, 2010.

[57] E. Koutroulis, D. Kolokotsa, A. Potirakis, and K. Kalaitzakis, "Methodology for optimal sizing of stand-alone photovoltaic/wind-generator systems using genetic algorithms," *Solar Energy*, vol. 80, no. 9, pp. 1072 – 1088, 2006.

[58] E. Mauky, S. Weinrich, H.-J. Nägele, H. F. Jacobi, J. Liebetrau, and M. Nelles, "Model predictive control for demand-driven biogas production in full scale," *Chemical Engineering & Technology*, 2016.

[59] M. Khalid and A. Savkin, "A model predictive control approach to the problem of wind power smoothing with controlled battery storage," *Renewable Energy*, vol. 35, no. 7, pp. 1520–1526, 2010.

[60] J. P. Torreglosa, P. García, L. M. Fernández, and F. Jurado, "Energy dispatching based on predictive controller of an off-grid wind turbine/photovoltaic/hydrogen/battery hybrid system," *Renewable Energy*, vol. 74, pp. 326–336, 2015.

[61] IEA, "Energy supply security 2014," 2014. `https://www.iea.org/publications/freepublications/publication/ENERGYSUPPLYSECURITY2014.pdf`.

[62] IEA, "Oil & gas security 2012, the netherlands," 2012. `https://www.iea.org/publications/freepublications/publication/OilGasSecurityNL2012.pdf`.

[63] G. Notton, M. Muselli, P. Poggi, and A. Louche, "Decentralized wind energy systems providing small electrical loads in remote areas," *International journal of energy research*, vol. 25, no. 2, pp. 141–164, 2001.

[64] Z. Yang, "Optimization and simulation of hybrid renewable energy system for urban building clusters," 2016.

[65] A. Chauhan and R. Saini, "A review on integrated renewable energy system based power generation for stand-alone applications: configurations, storage options, sizing methodologies and control," *Renewable and Sustainable Energy Reviews*, vol. 38, pp. 99–120, 2014.

[66] J. Seguro and T. Lambert, "Modern estimation of the parameters of the weibull wind speed distribution for wind energy analysis," *Journal of Wind Engineering and Industrial Aerodynamics*, vol. 85, no. 1, pp. 75–84, 2000.

[67] B. Grieser, Y. Sunak, and R. Madlener, "Economics of small wind turbines in urban settings: An empirical investigation for germany," *Renewable Energy*, vol. 78, pp. 334–350, 2015.

[68] S. Heier, *Windkraftanlagen: Systemauslegung, Netzintegration und Regelung*. Springer-Verlag,

2009.

[69] F. A. Mohamed *et al.*, "Microgrid modelling and online management," 2008.

[70] J. R. Andreesen, H. Bahl, and G. Gottschalk, "Introduction to the physiology and biochemistry of the genus $clostridium$," in *Clostridia*, pp. 27–62, Springer, 1989.

[71] M. J. McInerney, "Anaerobic hydrolysis and fermentation of fats and proteins," *Biology of anaerobic microorganisms*, vol. 38, pp. 373–415, 1988.

[72] L. G. Ljungdahl, J. Hugenholtz, and J. Wiegel, "Acetogenic and acid-producing $clostridia$," in *Clostridia*, pp. 145–191, Springer, 1989.

[73] L.-M. Whang, C.-J. Hsiao, and S.-S. Cheng, "A dual-substrate steady-state model for biological hydrogen production in an anaerobic hydrogen fermentation process," *Biotechnology and bioengineering*, vol. 95, no. 3, pp. 492–500, 2006.

[74] B. James and F. Ollis David, *Biochemical engineering fundamentals*. Mc Grow Hill Book Company, 1986.

[75] D. S. Clark and H. W. Blanch, *Biochemical engineering*. CRC Press, 1997.

[76] D. J. Batstone, J. Keller, I. Angelidaki, S. Kalyuzhnyi, S. Pavlostathis, A. Rozzi, W. Sanders, H. Siegrist, and V. Vavilin, "The IWA anaerobic digestion model no 1 (ADM1)," *Water Science and Technology*, vol. 45, no. 10, pp. 65–73, 2002.

[77] I. Valdez-Vazquez, E. Ríos-Leal, F. Esparza-García, F. Cecchi, and H. M. Poggi-Varaldo, "Semi-continuous solid substrate anaerobic reactors for H_2 production from organic waste: mesophilic versus thermophilic regime," *International Journal of Hydrogen Energy*, vol. 30, no. 13, pp. 1383–1391, 2005.

[78] T. Eggeman and R. T. Elander, "Process and economic analysis of pretreatment technologies," *Bioresource technology*, vol. 96, no. 18, pp. 2019–2025, 2005.

[79] B. D. James, G. N. Baum, J. Perez, and K. N. Baum, "Technoeconomic boundary analysis of biological pathways to hydrogen production," *US Department of Energy: September*, 2009.

[80] G. Gahleitner, "Hydrogen from renewable electricity: An international review of power-to-gas pilot plants for stationary applications," *International Journal of Hydrogen Energy*, vol. 38, no. 5, pp. 2039–2061, 2013.

[81] J. M. Maciejowski, *Predictive control: with constraints*. Pearson education, 2002.

[82] M. Arnold and G. Andersson, "Model predictive control of energy storage including uncertain forecasts," in *Power Systems Computation Conference (PSCC), Stockholm, Sweden*, Citeseer, 2011.

[83] M. Diehl, H. J. Ferreau, and N. Haverbeke, "Efficient numerical methods for nonlinear MPC and moving horizon estimation," in *Nonlinear model predictive control*, pp. 391–417, Springer, 2009.

[84] G. Pannocchia, J. B. Rawlings, and S. J. Wright, "Fast, large-scale model predictive control by partial enumeration," *Automatica*, vol. 43, no. 5, pp. 852–860, 2007.

[85] B. Fabiano and P. Perego, "Thermodynamic study and optimization of hydrogen production by enterobacter aerogenes," *International Journal of Hydrogen Energy*, vol. 27, no. 2, pp. 149–156, 2002.

[86] K. P. Capaldo and S. N. Pandis, "Dimethylsulfide chemistry in the remote marine atmosphere: Evaluation and sensitivity analysis of available mechanisms," *Journal of Geophysical Research: Atmospheres*, vol. 102, no. D19, pp. 23251–23267, 1997.

[87] S. Van Ginkel and B. E. Logan, "Inhibition of biohydrogen production by undissociated acetic and butyric acids," *Environmental science & technology*, vol. 39, no. 23, pp. 9351–9356, 2005.

[88] KNMI, "Uurgegevens van het weer in nederland per schiphol." http://www.knmi.nl/nederland-nu/klimatologie/uurgegevens.

[89] GemeenteAmsterdam, "Gemeente amsterdam onderzoek, informate en statistiek." http://www.ois.amsterdam.nl/feiten-en-cijfers/stadsdelen.

[90] Wikipedia, "Wikipedia nieuw-west." https://nl.wikipedia.org/wiki/Nieuw-West_(Amsterdam).

[91] Eurostat, "Municipal waste generation and treatment." http://ec.europa.eu/eurostat/tgm/refreshTableAction.do?tab=table&plugin=1&pcode=tsdpc240&language=en.

[92] CBS, "Halve ton huisvuil per persoon." https://www.cbs.nl/nl-nl/nieuws/2000/14/halve-ton-huisvuil-per-persoon.

[93] Windenergy, "Skystrem 3.7." http://www.windenergy.com/products/skystream/skystream-3.7.

[94] Skystreamenergy, "Introduction - skystrem 3.7." http://www.eco-distributing.com/Skystream_Intro_FAQ.pdf.

[95] xzeres, "xzeres skystrem 3.7." http://www.xzeres.com/wind-turbine-products/xzeres-skystream-3-7wind-turbine/.

[96] SinoVoltaices, "Standard test conditions (stc): definition and problems." http://sinovoltaics.com/learning-center/quality/standard-test-conditions-stc-definition-and-problems/.

[97] E. Skoplaki and J. Palyvos, "On the temperature dependence of photovoltaic module electrical performance: A review of efficiency/power correlations," *Solar energy*, vol. 83, no. 5, pp. 614–624, 2009.

[98] R. Bhattacharya, J. Hiltner, W. Batchelor, M. Contreras, R. Noufi, and J. Sites, "15.4% CuIn 1- x Ga x Se 2-based photovoltaic cells from solution-based precursor films," *Thin Solid Films*, vol. 361, pp. 396–399, 2000.

[99] P.-L. Chang and C.-W. Hsu, "Value analysis for commercialization of fermentative hydrogen production from biomass," *international journal of hydrogen energy*, vol. 37, no. 20, pp. 15746–15752, 2012.

[100] C. Chen, C. Lin, and J. Chang, "Kinetics of hydrogen production with continuous anaerobic cultures utilizing sucrose as the limiting substrate," *Applied Microbiology and Biotechnology*, vol. 57, no. 1-2, pp. 56–64, 2001.

[101] F. Fernández, J. Villaseñor, and D. Infantes, "Kinetic and stoichiometric modelling of acidogenic fermentation of glucose and fructose," *biomass and bioenergy*, vol. 35, no. 9, pp. 3877–3883, 2011.

[102] T. Yigit and O. F. Selamet, "Mathematical modeling and dynamic simulink simulation of high-pressure PEM electrolyzer system," *International Journal of Hydrogen Energy*, vol. 41, no. 32, pp. 13901–13914, 2016.

[103] FuelCellEnergy, "DFC4000™,"

[104] DutchAmsterdam, "A'dam lookout — amsterdam 360° panorama observation deck." http://www.dutchamsterdam.nl/4321-adam-toren.

[105] CBS, "Natural gas balance sheet," 2014. http://statline.cbs.nl/Statweb/publication/?DM=SLEN&PA=00372eng&D1=8&D2=596,611,623-624,626-628&LA=EN&HDR=G1&STB=T&VW=T.

[106] NAM, "NAM Underground Gas Storage," 2011. http://www.nam.nl/content/dam/shell/static/nam/downloads/pdf/nam-gasbuffer-engkl.pdf.

[107] KBBNet, "Zuidwending underground gas storage aardgasbuffer," 2009. http://www.kbbnet.de/wp-content/uploads/2011/05/110201-Zuidwending.pdf.

[108] CBS, "More electricity generated to meet higher foreign demand," 2015. https://www.cbs.nl/en-gb/news/2015/17/more-electricity-generated-to-meet-higher-foreign-demand.

[109] CBS, "Energy balance sheet," 2014. http://statline.cbs.nl/Statweb/publication/?DM=SLEN&PA=83140eng&D1=a&D2=0-1,11,34-35,49-50&D3=24&HDR=G2,G1&STB=T&VW=T.

[110] J.-G. Bartaire, R. Bauerschmidt, T. Ohman, Z. TIHANYI, H. ZEINHOFER, J. F. SCOWCROFT, V. DE JANEIRO, H. KRUGER, H.-J. MEIER, D. OFFERMANN, and U. LANGNICKEL, "Efficiency in electricity generation," tech. rep., EURELECTRIC "Preservation of Resources" Working Group's "Upstream" Sub-Group in collaboration with VGB, 2003.

[111] S.-K. Han and H.-S. Shin, "Performance of an innovative two-stage process converting food waste to hydrogen and methane," *Journal of the Air & Waste Management Association*, vol. 54, no. 2, pp. 242–249, 2004.

[112] A. Shah, L. Favaro, L. Alibardi, L. Cagnin, A. Sandon, R. Cossu, S. Casella, and M. Basaglia, "$bacillus sp.$ strains to produce bio-hydrogen from the organic fraction of municipal solid waste," *Applied Energy*, vol. 176, pp. 116–124, 2016.

Appendix A Plottings

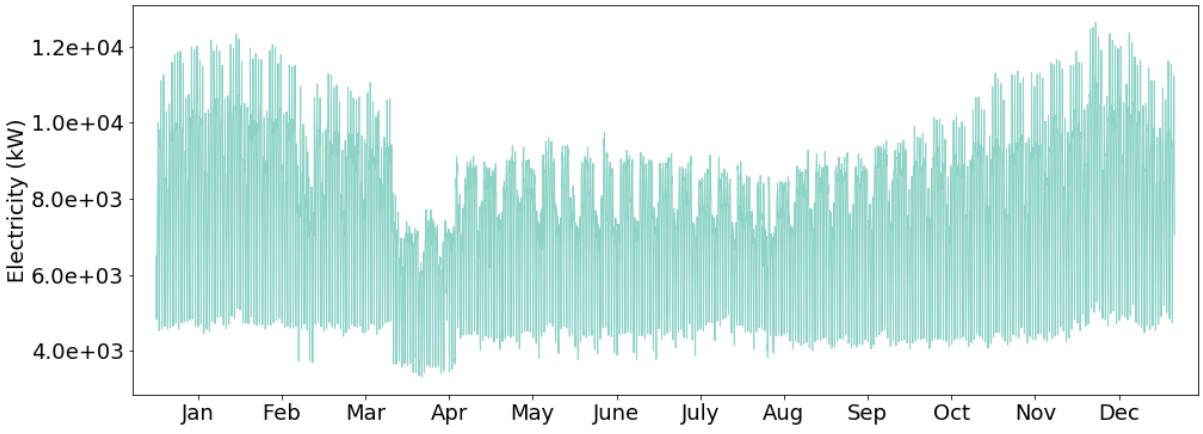

Figure A.1: Hourly electricity demand of Slotermeer in 2014

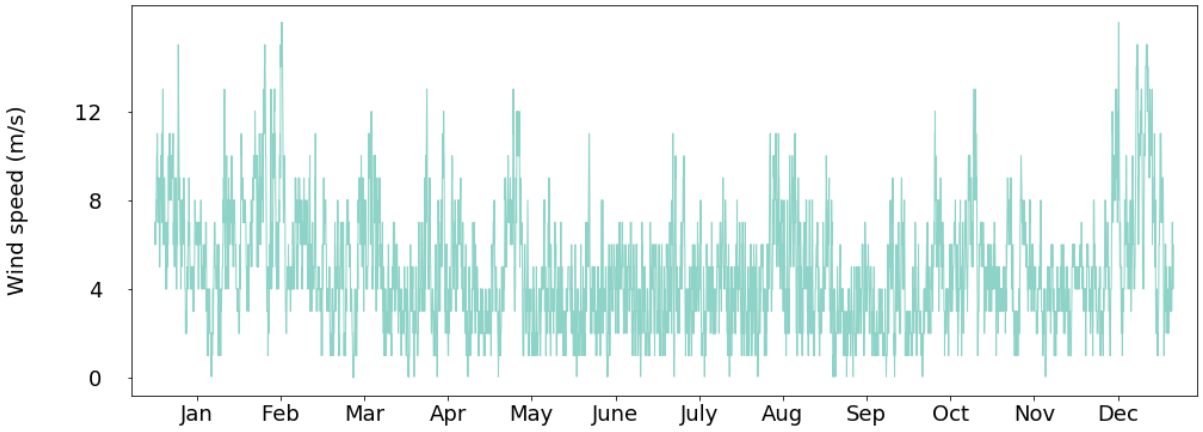

Figure A.2: Hourly wind speed at Slotermeer in 2014

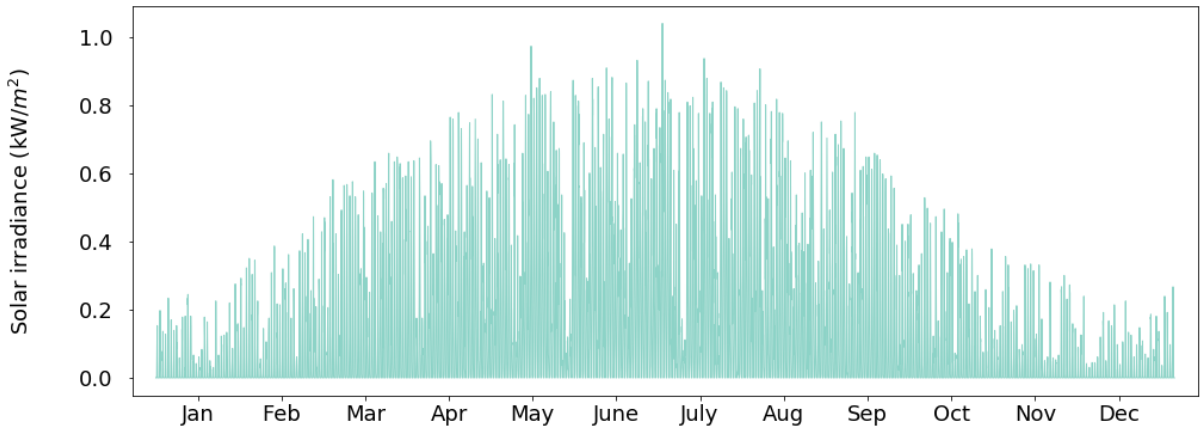

Figure A.3: Hourly solar irradiance at Slotermeer in 2014

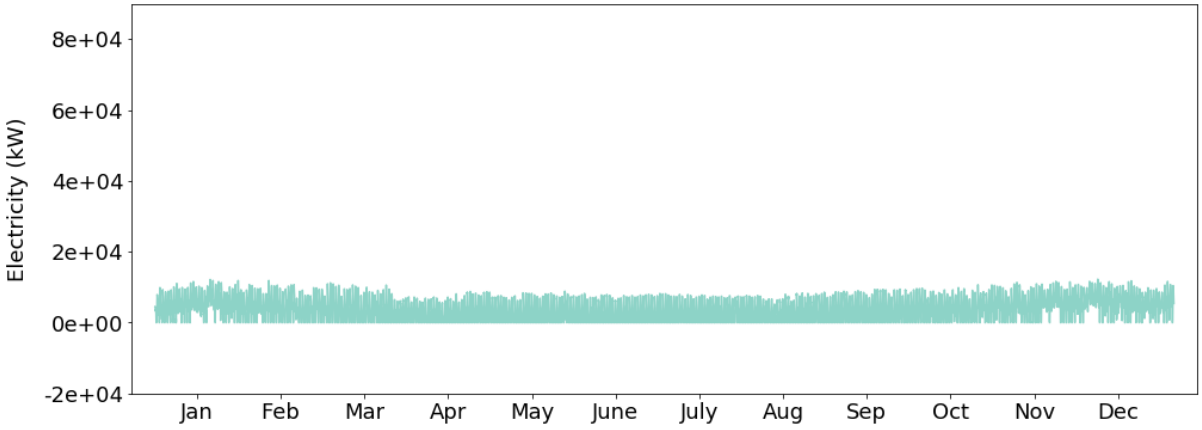

Figure A.4: Hourly electricity generated by fuel cell for Scenario 1, 2 & 3

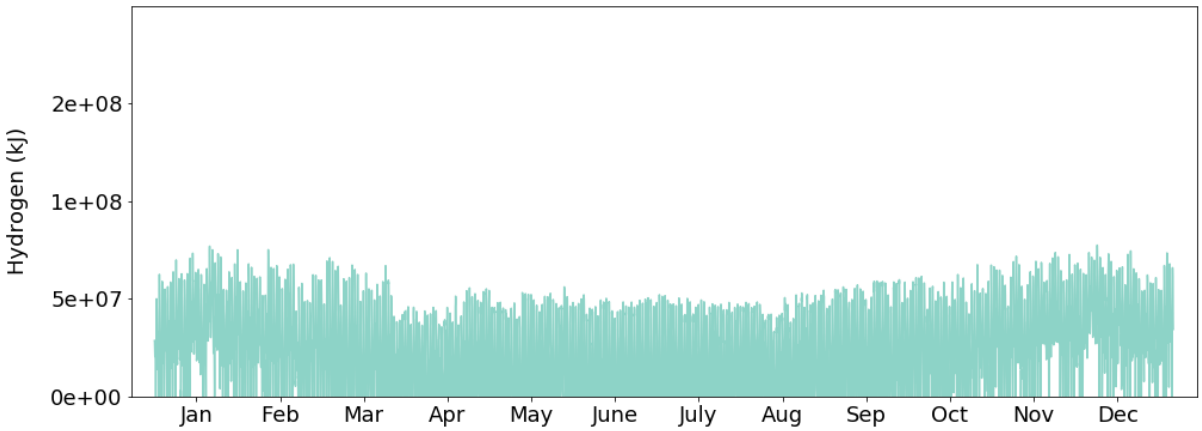

Figure A.5: Hourly hydrogen consumed by fuel cell for Scenario 1, 2 & 3

A.1 Plottings of Scenario without MPC

Figure A.6: Biomass concentration in the fermenter when $G_{0,B}$ = 27.23 g/L, without MPC

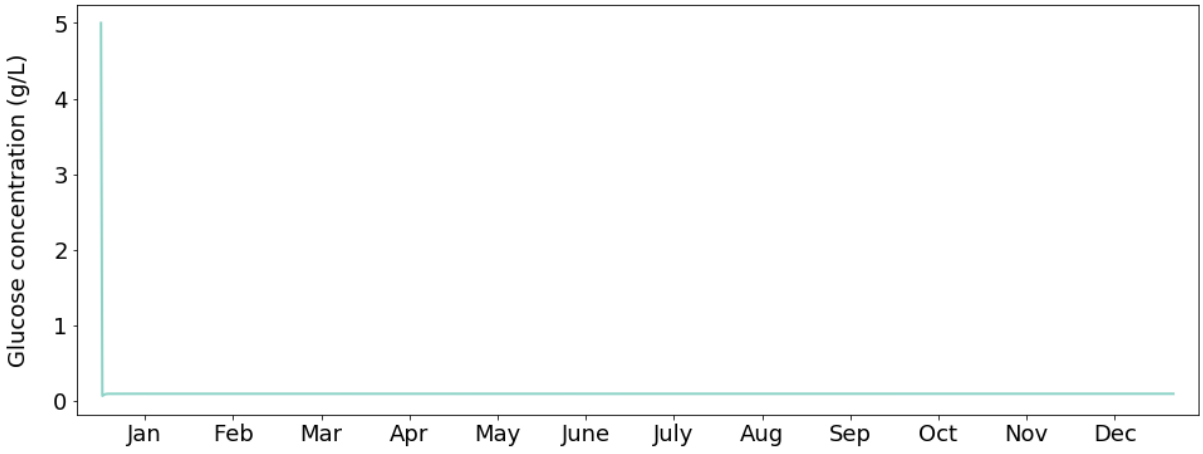

Figure A.7: Glucose concentration in the fermenter when $G_{0,B}$ = 27.23 g/L, without MPC

A.2 Plottings of Scenario 1

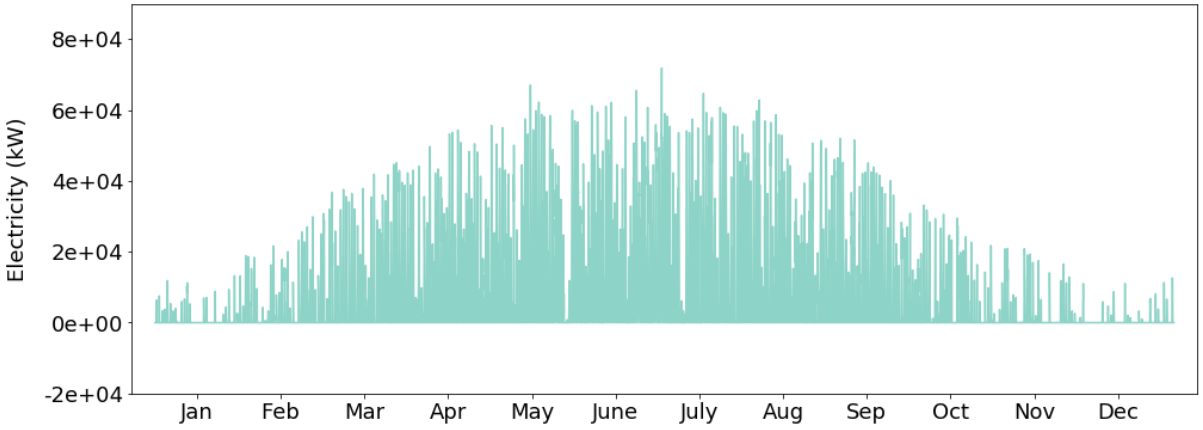

Figure A.8: Hourly electricity consumed by electrolyzer for Scenario 1 when $G_{0,B}$ = 27.23 g/L

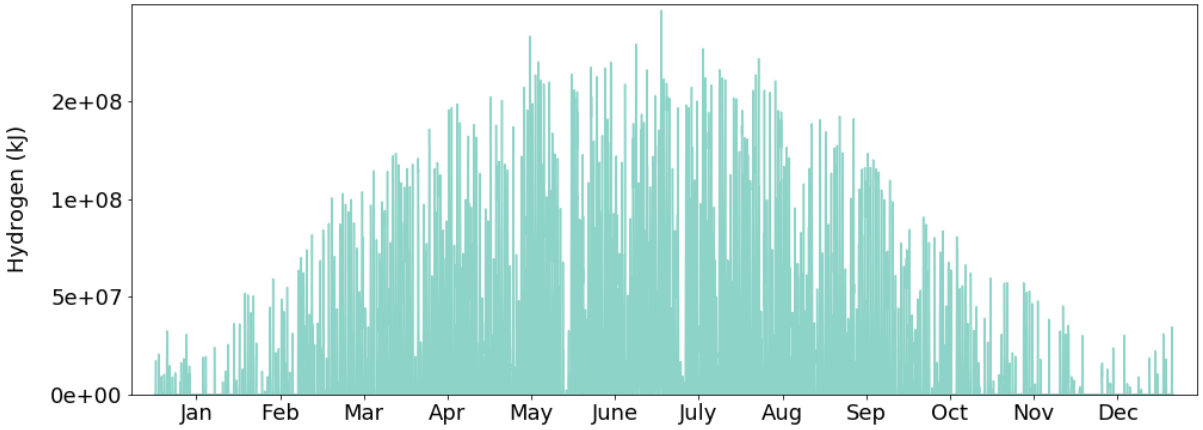

Figure A.9: Hourly hydrogen generated by electrolyzer for Scenario 1 when $G_{0,B}$ = 27.23 g/L

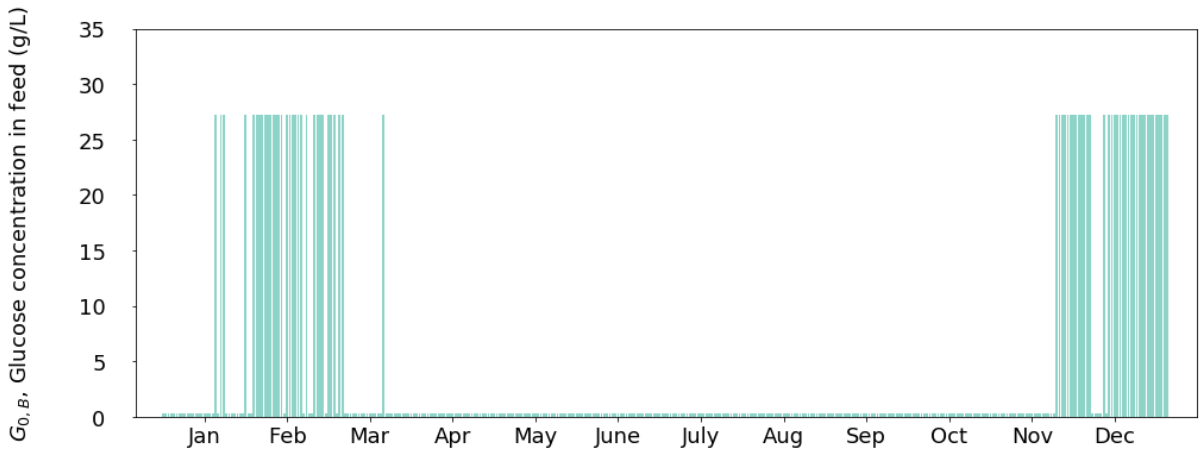

Figure A.10: Hourly glucose concentration in feed for Scenario 1 when $G_{0,B}$ = 27.23 g/L

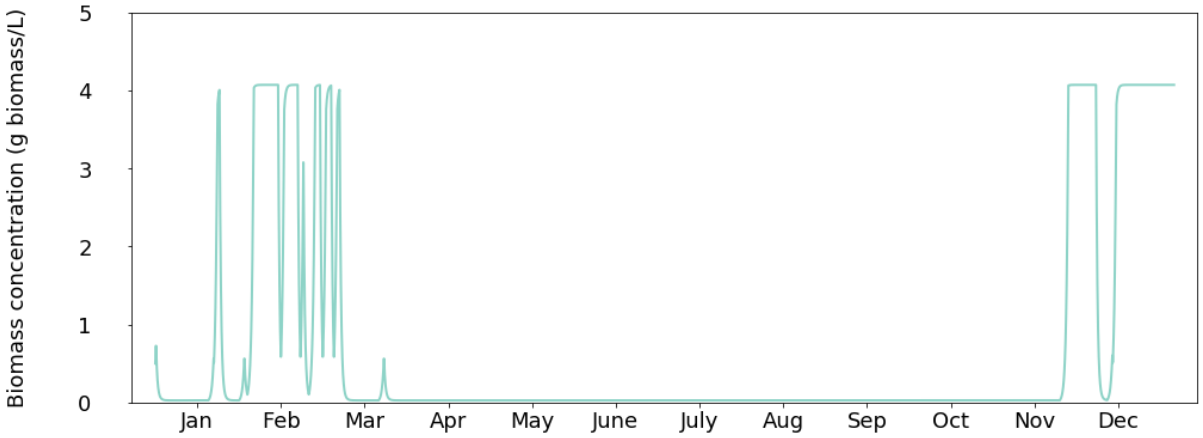

Figure A.11: Biomass concentration in the fermenter for Scenario 1 when $G_{0,B}$ = 27.23 g/L

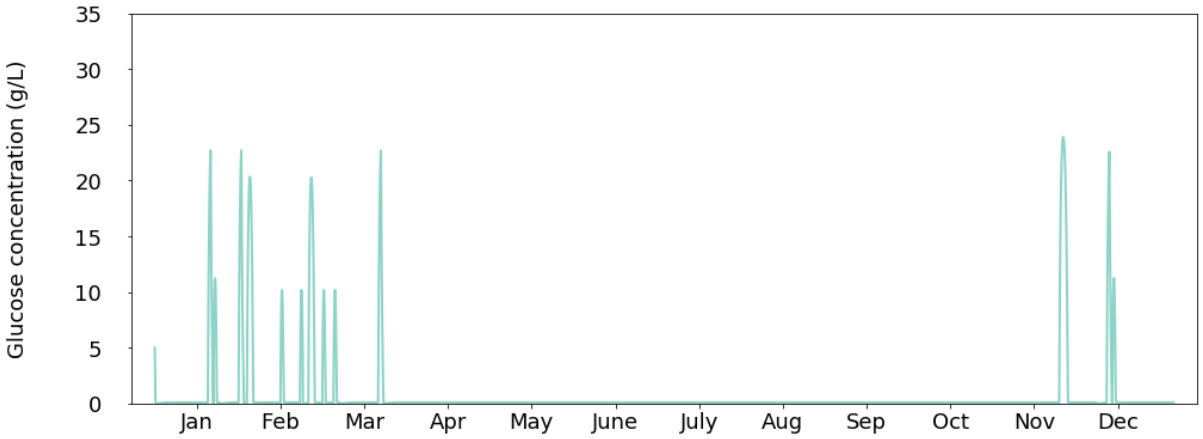

Figure A.12: Glucose concentration in the fermenter for Scenario 1 when $G_{0,B}$ = 27.23 g/L

A.3 Plottings of Scenario 2

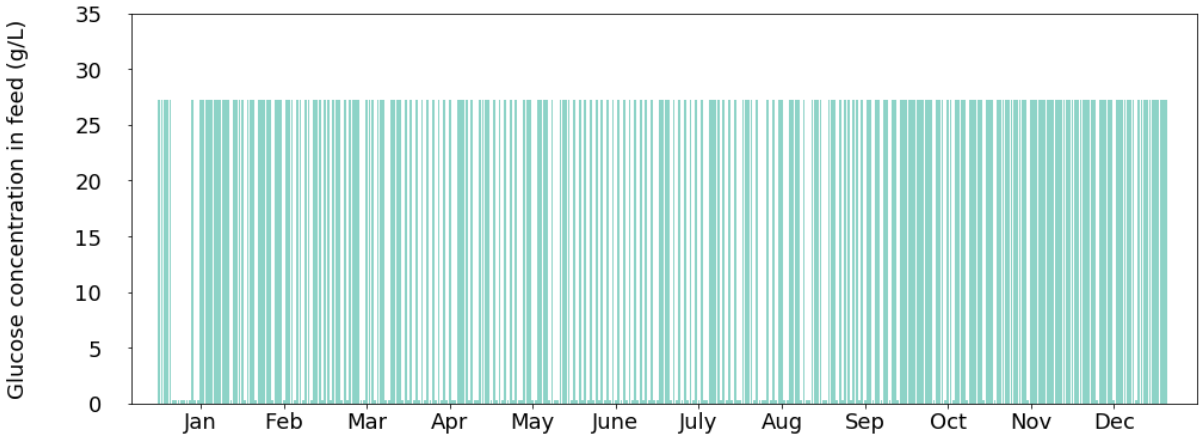

Figure A.13: Hourly glucose concentration in feed for Scenario 2 when $G_{0,B}$ = 27.23 g/L

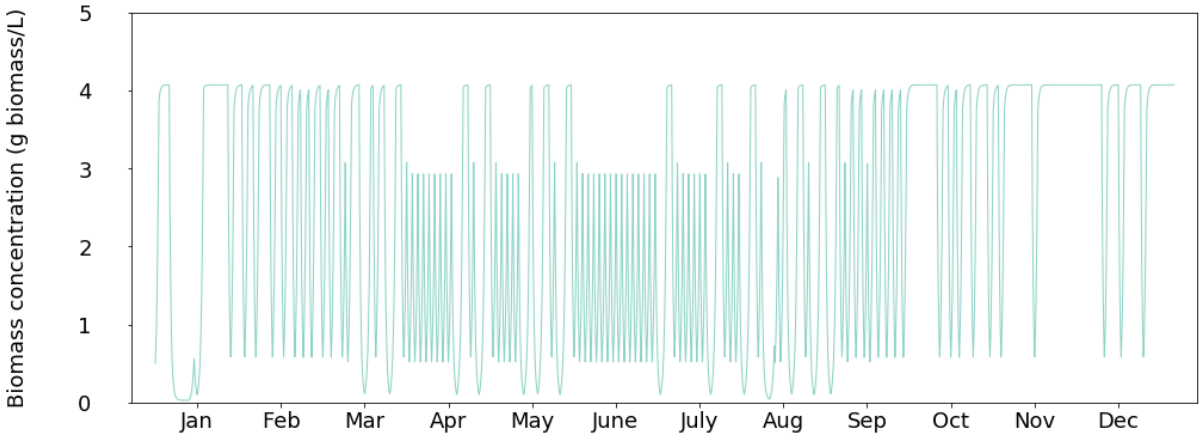

Figure A.14: Biomass concentration in the fermenter for Scenario 2 when $G_{0,B}$ = 27.23 g/L

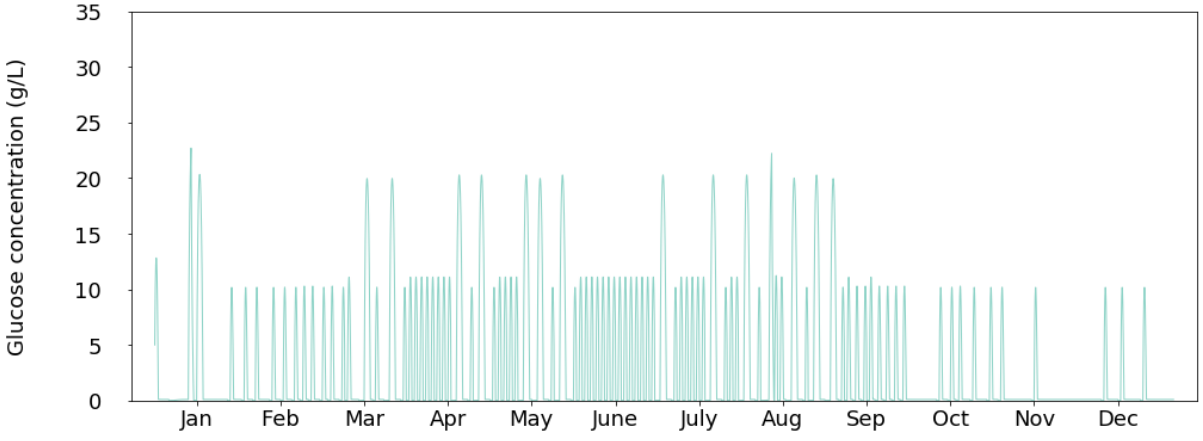

Figure A.15: Glucose concentration in the fermenter for Scenario 2 when $G_{0,B}$ = 27.23 g/L

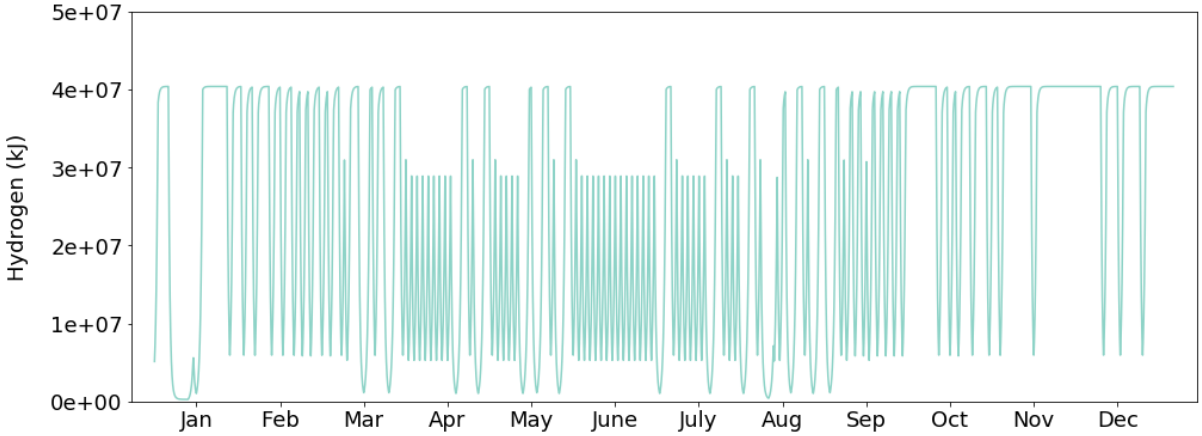

Figure A.16: Hourly H_2 produced via fermentation for Scenario 2 when $G_{0,B}$ = 27.23 g/L

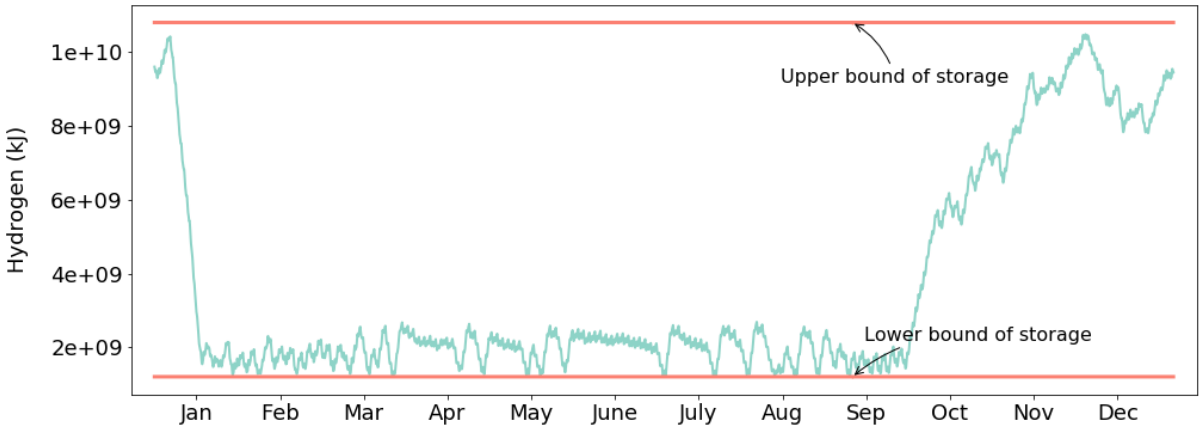

Figure A.17: Hydrogen storage level for Scenario 2 when $G_{0,B}$ = 27.23 g/L

A.4 Plottings of Scenario 3

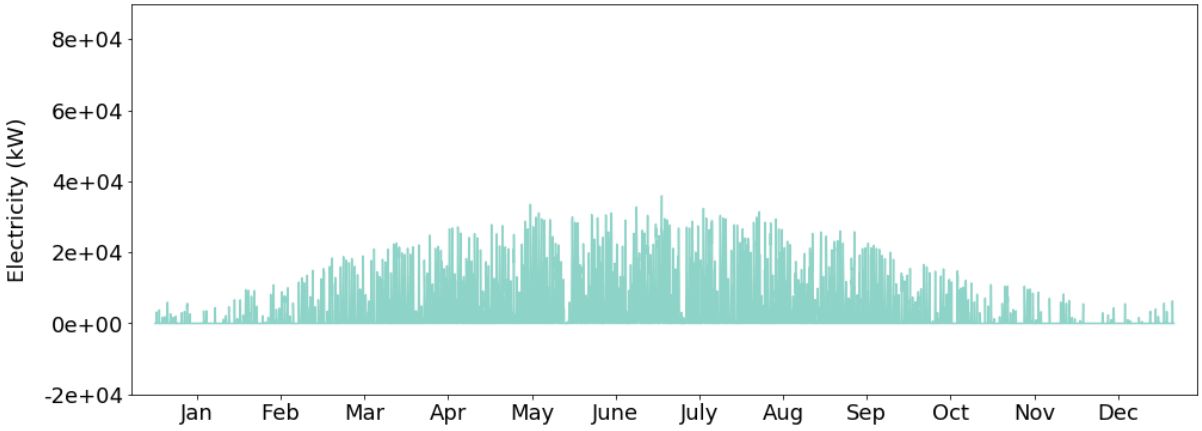

Figure A.18: Hourly electricity consumed by electrolyzer for Scenario 3 when $G_{0,B}$ = 27.23 g/L

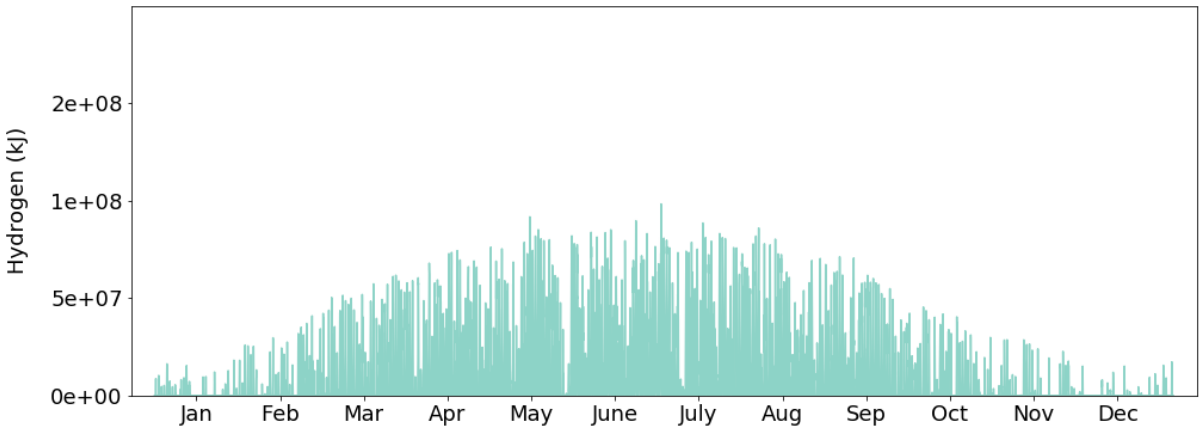

Figure A.19: Hourly hydrogen generated by electrolyzer for Scenario 3 when $G_{0,B}$ = 27.23 g/L

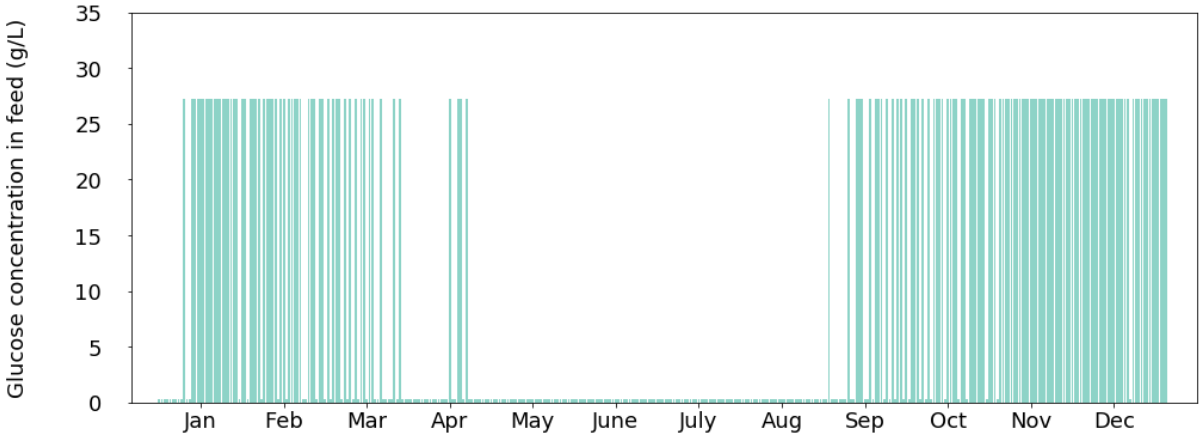

Figure A.20: Hourly glucose concentration in feed for Scenario 3 when $G_{0,B}$ = 27.23 g/L

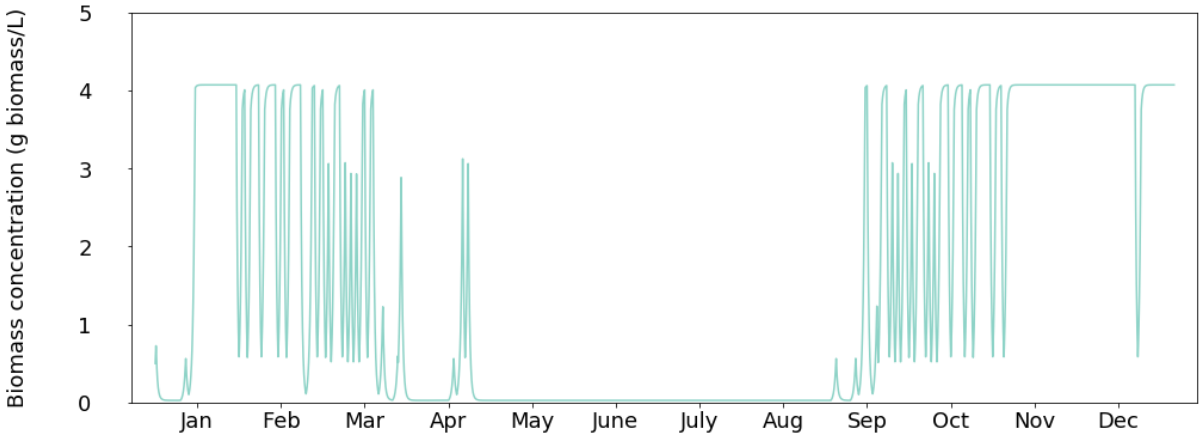

Figure A.21: Biomass concentration in the fermenter for Scenario 3 when $G_{0,B}$ = 27.23 g/L

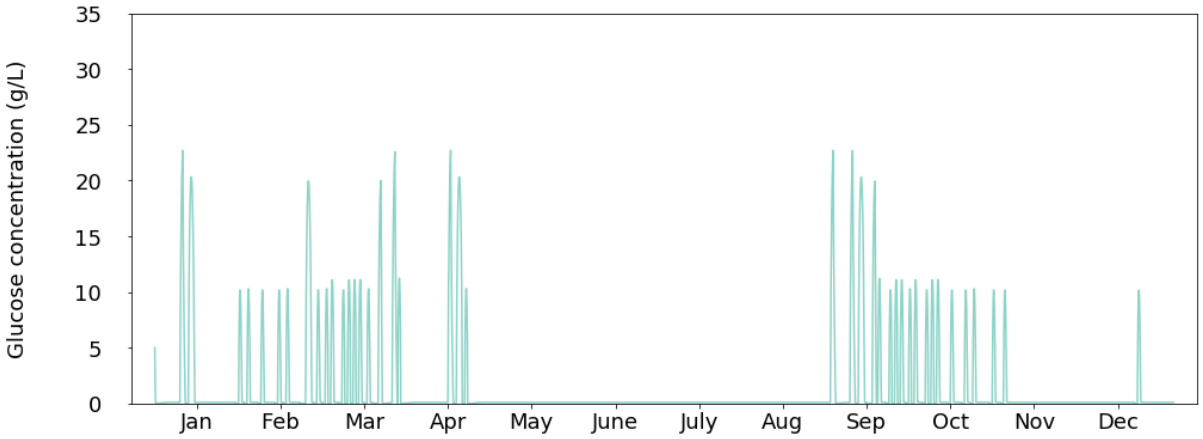

Figure A.22: Glucose concentration in the fermenter for Scenario 3 when $G_{0,B}$ = 27.23 g/L

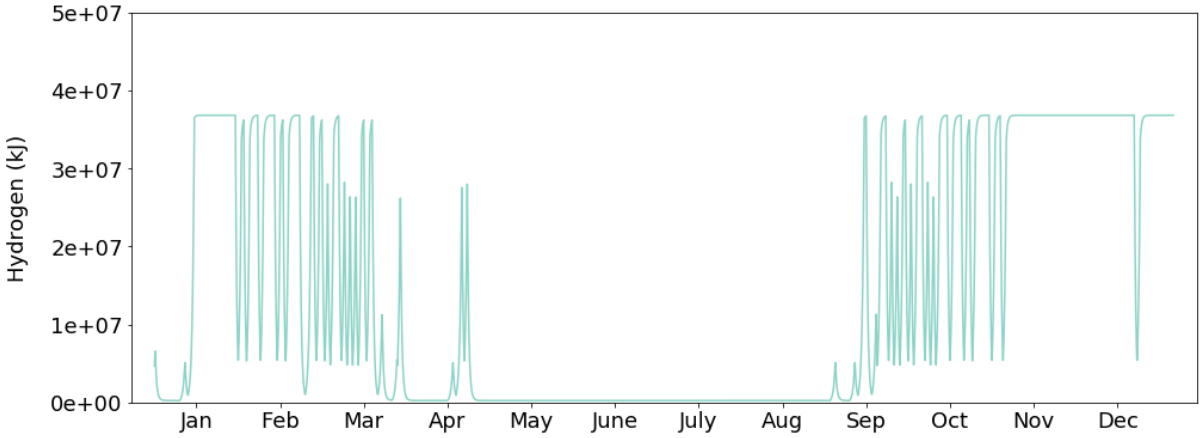

Figure A.23: Hourly H_2 produced via fermentation for Scenario 3 when $G_{0,B}$ = 27.23 g/L

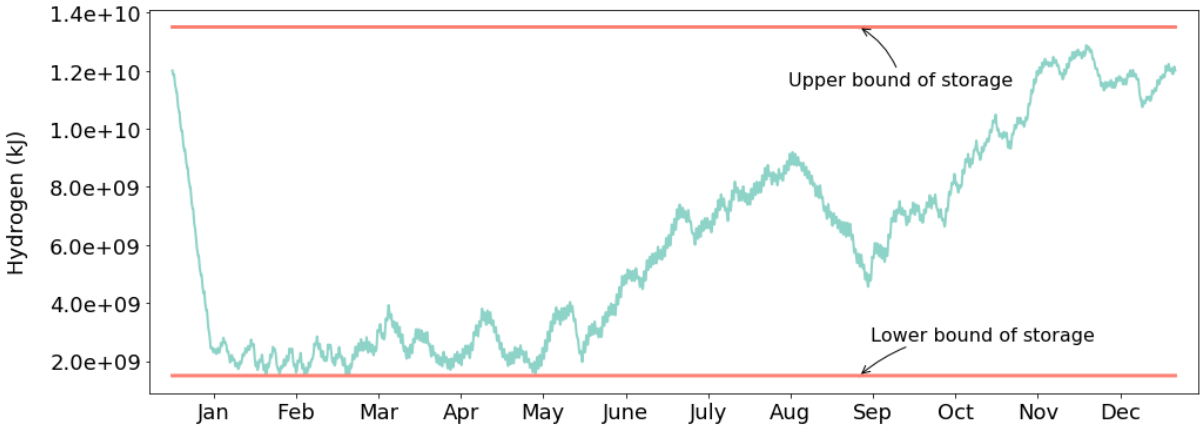

Figure A.24: Hydrogen storage level for Scenario 3 when $G_{0,B}$ = 27.23 g/L

Appendix B Tables

Table B.1: Complete comparison among Scenario 1, 2 & 3

Component size/capacity	**Unit**	**Scenario 1**	**Scenario 2**	**Scenario 3**
H_2 storage tank	m^3	10,690	1,550	1,940
Fermentation tank	m^3	2,820	4,000	3,650
Electrolyzer	m^3H_2/h	15,390	0	7,690
Fuel cell	MW	12	12	12
System outcomes	**Unit**	**Scenario 1**	**Scenario 2**	**Scenario 3**
GFT consumption	ton	34,070	171,460	98,630
Bio-H_2 production	mol	1.43e+08	7.11e+08	4.28e+08
Operating cost	€/year	2.89e+06	4.72e+06	3.81e+06

Appendix C Calculations

Conversion between glucose and GFT waste

Assuming H_2 yield obtained from [44] (180 ml H_2/g TVS) and [77] (3.2 mol H_2/mol hexose) are close, the following equation exists:

$$180\ [\text{ml } H_2/\text{g TVS}] = 3.2\ [\text{mol } H_2/\text{mol hexose}]$$

with 1 mol H_2 = 22.4 L H_2, the relation between TVS and hexose can be built:

$$1\ [\text{g TVS}] <=> 2.51 \times 10^{-3}\ [\text{mol hexose}]$$

The total volatile solids takes up 93% of the total solids which is assumed to be the dried mixture of organic fraction of municipal solid waste (OFMSW) and sludge [112, 44]. Thus:

$$1.0753\ [\text{g mixture}_{DW}] <=> 2.51 \times 10^{-3}\ [\text{mol hexose}]$$

The moisture content of the mixture is assumed to be 70%:

$$3.5842\ [\text{g mixture}] <=> 2.51 \times 10^{-3}\ [\text{mol hexose}]$$

The composition of GFT waste in the mixture is 46.3% [44]:

$$1.6595\ [\text{g GFT}] <=> 2.51 \times 10^{-3}\ [\text{mol hexose}]$$

The hexose is assumed to be glucose, thus the relation between GFT and contained glucose can be estimated as:

$$1\ [\text{g GFT}] <=> 0.2723\ [\text{g glucose}]$$